Volume 9
Number 35
21 September 2021
Pages 6921–7280

Journal of Materials Chemistry B

Materials for biology and medicine

rsc.li/materials-b

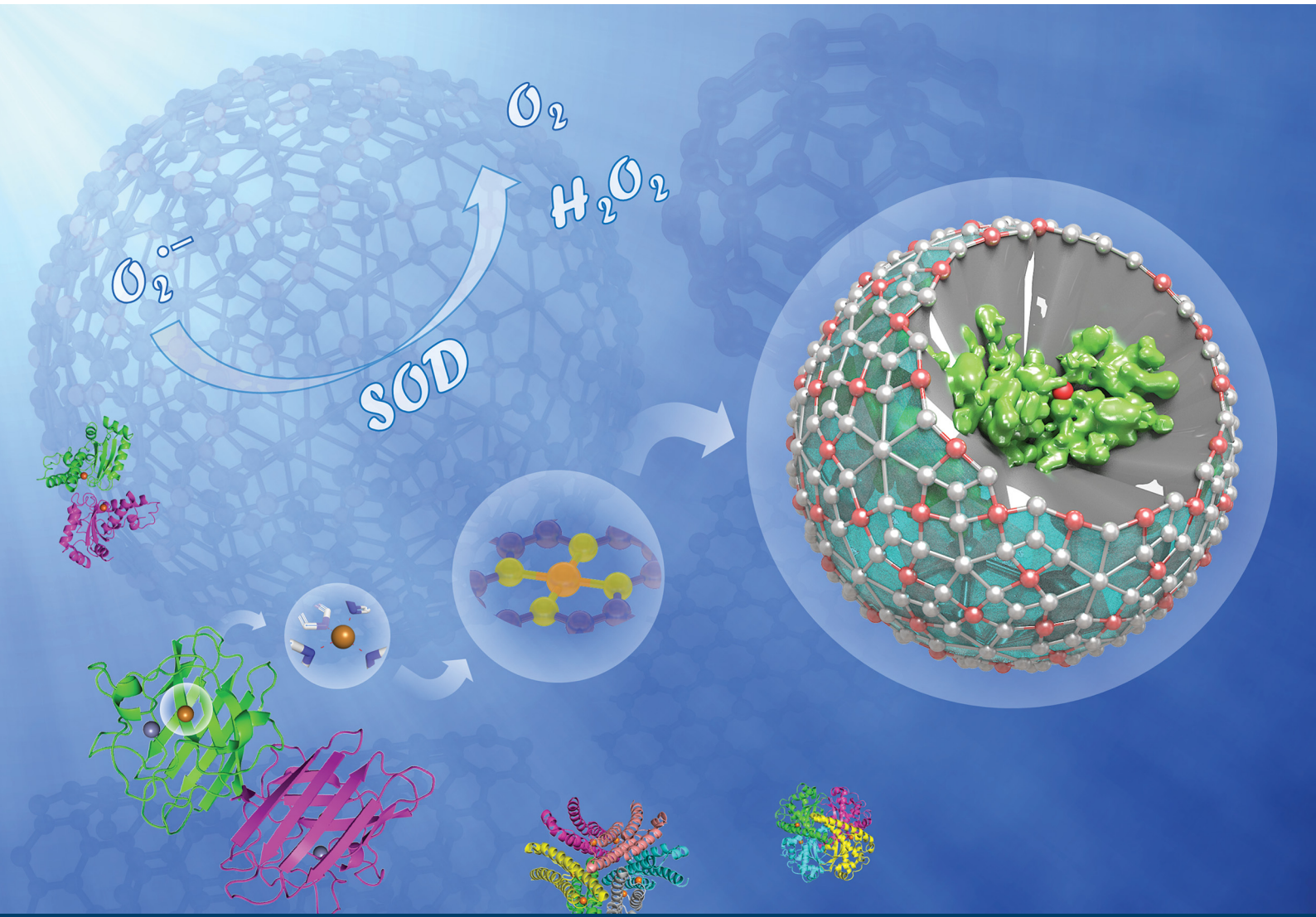

Themed issue: Emerging Investigators 2021

ISSN 2050-750X

ROYAL SOCIETY OF CHEMISTRY

REVIEW ARTICLE
Xiyun Yan, Kelong Fan *et al.*
Superoxide dismutase nanozymes: an emerging star for anti-oxidation

Indexed in Medline!

Journal of Materials Chemistry B

ROYAL SOCIETY OF CHEMISTRY

REVIEW

View Article Online
View Journal | View Issue

Cite this: *J. Mater. Chem. B*, 2021, **9**, 6939

Superoxide dismutase nanozymes: an emerging star for anti-oxidation

Hanqing Zhao,†[ab] Ruofei Zhang,†[ab] Xiyun Yan*[abc] and Kelong Fan*[abc]

Superoxide dismutases (SODs) are a group of metalloenzymes that catalyze the dismutation of superoxide radicals ($O_2^{\bullet -}$) into hydrogen peroxide (H_2O_2) and oxygen (O_2). As the first line of defense against reactive oxygen species (ROS)-mediated damage, SODs are expected to play an important role in the treatment of oxidative stress-related diseases. However, the clinical applications of SODs have been severely limited by their structural instability and high cost. Compared with natural enzymes, nanozymes, nanomaterials with enzyme-like activity, are more stable, and economical, can be easily modified and their activities can be adjusted. Due to their excellent characteristics, nanozymes have attracted widespread attention in recent years and are expected to become effective substitutes for natural enzymes in many application fields. Importantly, some nanozymes with SOD-like activity have been developed and proved to have a mitigating effect on diseases caused by oxidative stress. These studies on SOD-like nanozymes provide a feasible strategy for breaking through the dilemma of SOD clinical applications. However, at present, the specific catalytic mechanism of SOD-like nanozymes is still unclear, and many important issues need to be resolved. Although there are many comprehensive reviews to introduce the overall situation of the nanozyme field, the research on SOD-like nanozymes still lacks a systematic review. From the structure and mechanism of natural SOD enzymes to the structure and regulation of SOD-like nanozymes, and then to the measurement and application of nanozymes, this review systematically summarizes the recent progress in SOD-like nanozymes. The existing shortcomings and possible future research hotspots in the development of SOD-like nanozymes are summarized and prospected. We hope that this review would provide ideas and inspirations for further research on the catalytic mechanism and rational design of SOD-like nanozymes.

Received 1st April 2021,
Accepted 27th May 2021

DOI: 10.1039/d1tb00720c

rsc.li/materials-b

[a] *CAS Engineering Laboratory for Nanozyme, Key Laboratory of Protein and Peptide Pharmaceutical, Institute of Biophysics, Chinese Academy of Sciences, Beijing 100101, China. E-mail: fankelong@ibp.ac.cn, yanxy@ibp.ac.cn*
[b] *University of Chinese Academy of Sciences, Beijing 101408, China*
[c] *Nanozyme Medical Center, School of Basic Medical Sciences, Zhengzhou University, Zhengzhou 450052, Henan, China*
† Both authors contributed equally to this work.

Hanqing Zhao

Hanqing Zhao is currently a MS candidate at the Institute of Biophysics, Chinese Academy of Sciences (CAS) under the supervision of Prof. Xiyun Yan and Prof. Kelong Fan. She received her BS degree from Shenyang Pharmaceutical University in China in 2020. Her research interests focus on ferritin and nanozymes and their catalytic mechanism and biomedical applications.

Ruofei Zhang

Ruofei Zhang is currently a PhD candidate at the Institute of Biophysics, Chinese Academy of Sciences (CAS) under the supervision of Prof. Xiyun Yan and Prof. Kelong Fan. He received his BS degree from Wuhan University in China in 2016. His research focuses on the catalytic mechanism and application of nanozymes.

1. Introduction

Reactive oxygen species (ROS) are formed from incomplete reduction of oxygen molecules. As shown in Fig. 1, excessive production of ROS leads to oxidative stress, a harmful process that acts as an important mediator of cellular structural damage, especially lipid peroxidation and membrane damage, and protein and DNA oxidative damage.[15] Oxidative damage is a double-edged sword. On the one hand, it damages normal tissues and cells as mentioned above, while on the other hand, oxidative damage is able to induce cell senescence and apoptosis, which may be used for anti-tumor and antibacterial applications. Therefore, reasonable regulation of ROS is a promising strategy to treat a variety of redox related diseases. There are three main forms of ROS: superoxide radical ($O_2^{\bullet -}$), hydrogen peroxide (H_2O_2), and hydroxyl radical ($^{\bullet}OH$). Among them, $O_2^{\bullet -}$, the addition of an electron to dioxygen, is the principal one.[19] $O_2^{\bullet -}$ is produced in the mitochondria of cells mainly through metabolic processes or physical irradiation to "activate" oxygen, which further interacts with other molecules to produce "secondary" ROS.[20] $O_2^{\bullet -}$ is converted to H_2O_2 by superoxide dismutase (SOD), and then some transition metals (such as Fe^{2+}, Cu^{+}, *etc.*) may decompose H_2O_2 into highly toxic $^{\bullet}OH$ (Fenton reactions).[21] Therefore, regulating the amount of $O_2^{\bullet -}$ *in vivo* is very important for the treatment of ROS and oxidative stress-related diseases.

SOD has the ability to scavenge $O_2^{\bullet -}$,[23] which catalyzes the dismutation of $O_2^{\bullet -}$ to produce O_2 and H_2O_2 as shown in eqn (1)–(3):

$$M^{(n+1)+} + O_2^{\bullet -} \rightarrow M^{n+} + O_2 \quad (1)$$

$$M^{n+} + O_2^{\bullet -} (+ 2H^{+}) \rightarrow M^{(n+1)+} + H_2O_2 \quad (2)$$

$$\text{Overall: } O_2^{\bullet -} + O_2^{\bullet -} + 2H^{+} \rightarrow O_2 + H_2O_2 \quad (3)$$

Here, $M^{(n+1)+}$ represents the oxidized form of the metal and M^{n+} represents the reduced form of the metal. This mechanism is also known as the ping-pong effect because it involves the sequential reduction and oxidation of the metal centers.[24]

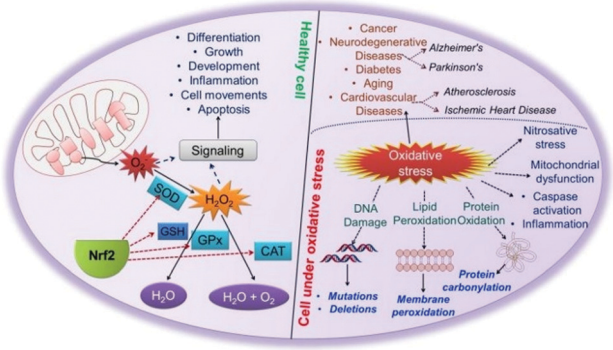

Fig. 1 Cellular antioxidant machinery and oxidative stress.[8] Reproduced with permission. Copyright 2009, The Royal Society of Chemistry.

Although natural enzymes have high catalytic efficiency, there are some limitations to their applications, including the high cost of preparation and purification, harsh reaction conditions, poor stability and so on. Based on this, a series of artificial enzymes have been developed to replace natural enzymes. Among them, nanozymes, a new generation of artificial enzymes, are currently a hot research topic. Nanozymes are a type of nanomaterial with intrinsic enzyme-like activity, which have unique characteristics compared with natural enzymes, such as low cost, high stability, easy production and preparation, easy tuning, *etc.* Table 1 compares the advantages and disadvantages of natural enzymes and nanozymes in detail. Fe_3O_4 magnetic nanoparticles were reported to have peroxidase-like activity in 2007, which was the first reported nanozyme.[26] Since then, the field of nanozymes has developed rapidly. Based on our statistical analysis of nanozyme-related publications from the Web of Science database, by January 2021, more than 1000 kinds of nanozymes have been reported, the composition of which involves 51 elements. There are more than 300 scientific researchers from

Xiyun Yan

Xiyun Yan is a professor at the Institute of Biophysics, a member of the Chinese Academy of Sciences, and the president of the Asian Biophysics Association. Her research interests include studying tumor biology, finding novel targets and developing new methods for tumor theranostics. Dr Yan introduced the concept of "nanozymes" (nanomaterials with enzyme-like characteristics) and used nanozymes for tumor diagnosis in combination with ferritin. Her work has been well recognized through honors such as the National Prize for Natural Science and Atlas Award by Elsevier.

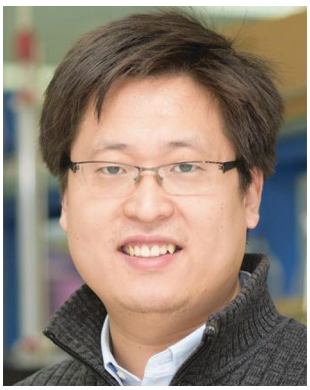

Kelong Fan

Kelong Fan received his PhD degree in cell biology from the Institute of Biophysics, Chinese Academy of Sciences in 2014. Then he stayed to further pursue 3 years of postdoc training and 2 years of associate professor work experience before attaining a full professor position in 2019. He is interested in exploring the novel functions and applications of nanozymes in biomedicine, with top priority to design functional nanozymes by learning from nature and to develop novel strategies for disease theranostics. He now serves as Associate Editor of Exploration and Guest Editor of Frontiers in Chemistry.

Table 1 Comparison of natural enzymes and nanozymes

	Natural enzymes	Nanozymes
Stability	Limited	High
Cost	High	Low
Production	Complex	Easy
Storage	Short term	Long term
Recyclable	No	Yes
Environments	Only mild	Could be harsh
Catalytic activity	Very high	High
Biocompatibility	Good	Limited
Selectivity	High	Limited

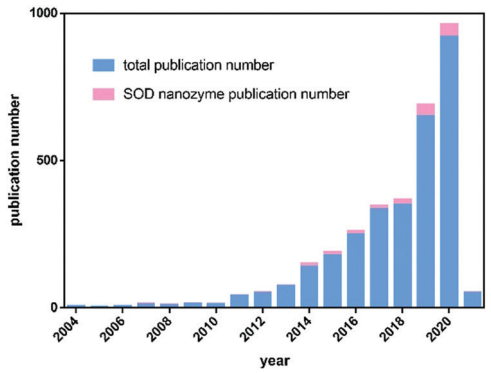

Fig. 2 The total publication number and SOD-like activity publication number of nanozymes. Statistics based on Web of Science until January 2021. Keywords: ''nanozyme*'' or [''nano*'' and (''*ase-like'' or ''*ase-mim*'' or ''enzyme mim*'' or ''enzyme like'')] not ''DNAzyme*''. We manually screened all the statistical studies and obtained these data.

31 countries exploring this field. Most nanozymes exhibited redox-related enzyme-like activities, mainly including the activities of oxidase, peroxidase, catalase and SOD. Among them, SOD-like nanozymes are the earliest discovered, but the least studied. There were more than 3000 nanozyme-related studies reported totally by January 2021, while there were only less than 200 studies related to SOD-like activity (Fig. 2). It is evident that, compared with other nanozymes, the development of SOD-like nanozymes was deficient. In addition, although there are some reviews that systematically summarize nanozymes, almost no specific review of SOD-like nanozymes has been reported. Considering the important prospects and practicality of SOD-like nanozymes in biomedical applications, it is necessary to make a comprehensive summary of its research to clarify its development and challenges. Thus, we summarize the advances of SOD-like nanozymes in the following sections. First, the structure and activity mechanism of natural SODs is briefly introduced. Then, based on the research of natural SODs, the catalytic mechanism and regulatory factors of the SOD-like activity of nanozymes are expounded. After that, the measurement methods and applications of SOD-like nanozymes in various fields are summarized. Finally, the challenges and prospects in the current development are put forward. We hope to deepen the understanding of the SOD-like activity of nanozymes and promote future research through this review (Scheme 1).

2. Structure and catalytic mechanism of natural SOD enzymes

Natural SODs, which are generally composed of proteins and metal cofactors, are considered to be necessary for aerobic cells. Natural SODs exist in most prokaryotic cells and some eukaryotic cells, and are widely present in various organelles. Based on different cofactors, natural SOD enzymes are divided into four types: copper-zinc SOD (CuZnSOD), manganese SOD (MnSOD), iron SOD (FeSOD), and nickel SOD (NiSOD).

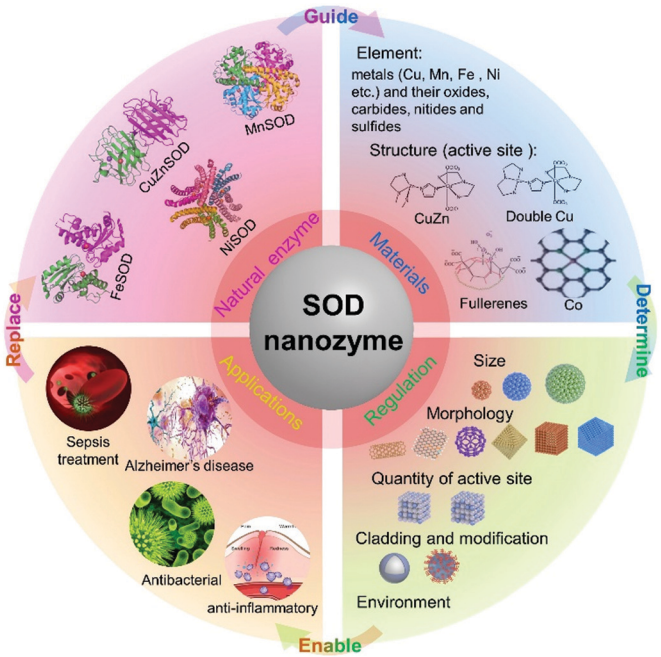

Scheme 1 Natural SOD guides the design, regulation and application of SOD nanozyme.

The structure and mechanism of these natural SOD enzymes are briefly introduced below.

2.1 Copper-zinc superoxide dismutase (CuZnSOD)

As shown in Fig. 3, the structure of natural CuZnSOD is composed of two subunits linked by histidine, each of which has an active center composed of metal atoms, Cu and Zn. In the active center, Cu acts as the catalytic site, while Zn maintains the stability of the enzyme.[27] During the catalytic reaction, Cu is alternatively reduced and oxidized in continuous encounters with $O_2^{\bullet -}$, changing between +2 and +1 valence states. As shown in eqn (4) and (5), $Cu^{2+}Zn^{2+}$SOD first adsorbs and binds $O_2^{\bullet -}$ and then mediates its oxidation. In this process, $Cu^{2+}Zn^{2+}$SOD turns into $Cu^{+}Zn^{2+}$SOD with slight changes in the structure while oxidizing $O_2^{\bullet -}$ to O_2. Then, $Cu^{+}Zn^{2+}$SOD combines with another molecule $O_2^{\bullet -}$, reducing it to H_2O_2 and returning to the original form of $Cu^{2+}Zn^{2+}$SOD.[28] In this process, copper must be exposed to the solvent outside the enzyme so that it can bind with the $O_2^{\bullet -}$ to initiate the reaction.[29–31]

$$Cu^{2+}Zn^{2+}SOD + O_2^{\bullet -} \rightarrow Cu^{+}Zn^{2+}SOD + O_2 \quad (4)$$

$$Cu^{+}Zn^{2+}SOD + O_2^{\bullet -} (+2H^{+}) \rightarrow Cu^{2+}Zn^{2+}SOD + H_2O_2 \quad (5)$$

The rate of catalytic reaction is related to the electrostatic attraction of negatively charged $O_2^{\bullet -}$ into the positively charged active center. Positively charged arginine near the active site greatly enhances electrostatic guidance. Once this arginine is mutated to uncharged isoleucine or negatively charged glutamic acid or aspartic acid, the catalytic efficiency (k_{cat}) of CuZnSOD decreases.[32] Another study showed that site-specific mutants that increase local positive charge such as changing negatively charged glutamic acid to glutamine near the active site produced more efficient enzymes than wild-type enzymes.[33] The role of zinc-bridging imidazole in CuZnSOD is to maintain the geometry of the copper coordination sphere, allow the rapid dissociation of the combined peroxide, and make CuZnSOD pH-independent.[34] Once the Zn is removed, the second reduction reaction (eqn (5)) in the dismutation reaction of Cu^{2+}apoSOD becomes pH-dependent.

2.2 Manganese superoxide dismutase (MnSOD)

Despite catalyzing a similar reaction, the active center structure of MnSOD is different from that of CuZnSOD. MnSOD has both dimer and tetramer structures. For prokaryotes (such as bacteria), MnSOD is in the dimer form, while the MnSOD of eukaryotic cells is usually in the tetramer form. Take the *human* MnSOD structure as an example (Fig. 4). There is one manganese active site in each subunit, and each manganese is coordinated with four protein ligands (three histidine residues and one aspartic acid residue) and a single-oxygen-containing molecule (H_2O or OH^-). Fig. 4(b) shows the inner sphere of the active center that interacts directly with manganese. The outer shell of the active center includes His30, Tyr34, Phe77, Trp78, Trp123, Gln143, Trp161, and Glu162, which are key residues to the highly efficient enzymatic activity.[35] The substrate is diffused to the active site through His30 and Tyr34 and binds with manganese ions. Phe77, Trp78, Trp123 and Trp161 form a hydrophobic cage to promote the interaction between the substrate and manganese ions. As shown in Fig. 5, manganese is caved in the lumen of the active site and forms a hydrogen bond network with the surrounding side chain residues such as Tyr34 and Gln143 and with two single-oxygen-containing molecules at the opening of the cavity.[36] The role of the hydrogen bond network is probably to promote proton transfer in the process of $O_2^{\bullet -}$ reduction to H_2O_2, and maintain the stability and catalytic activity of MnSOD. Like other SODs, the catalytic mechanism of MnSOD involves a cycle between Mn^{3+} and Mn^{2+}. However, due to the complexity of the structure, the catalytic mechanism of MnSOD involves more steps than other SODs and involves a series of proton transfers (eqn (6)–(9)).[24,36]

$$Mn^{3+}SOD(OH^-) + O_2^{\bullet -} (+ H^+) \rightarrow Mn^{2+}SOD(H_2O) + O_2 \quad (6)$$

$$Mn^{2+}SOD(H_2O) + O_2^{\bullet -} (+ H^+) \rightarrow Mn^{3+}SOD(OH^-) + H_2O_2 \quad (7)$$

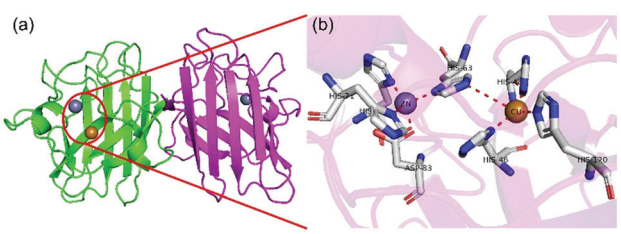

Fig. 3 Schematic illustration of CuZnSOD. (a) The structure and (b) active sites of *human* CuZnSOD (pdb ref: 1pu0). Picture created with PyMOL.

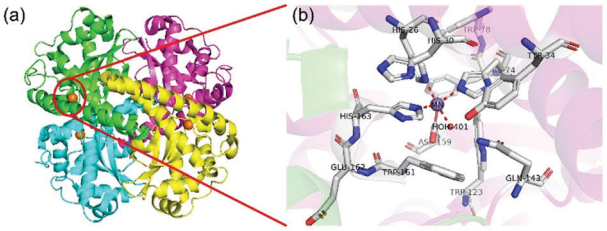

Fig. 4 Schematic illustration of MnSOD. (a) The structure and (b) active sites of *human* MnSOD (pdb ref: 1n0j). Picture created with PyMOL.

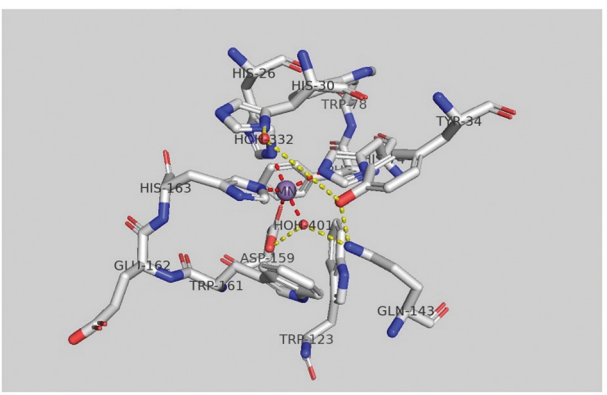

Fig. 5 Hydrogen bond network and superoxide-dependent proton transfer mechanism (pdb ref: 1n0j). Picture created with PyMOL.

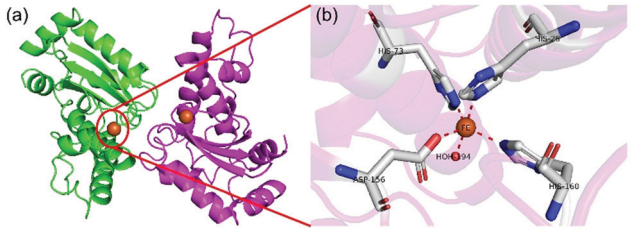

Fig. 6 Schematic illustration of FeSOD. (a) The structure and (b) active sites of *E. coli* FeSOD (pdb ref: 1isa). Picture created with PyMOL.

$$Mn^{2+}SOD(H_2O) + O_2^{\bullet -} \rightarrow Mn^{3+}SOD(H_2O) - O_2^{2-} \quad (8)$$

$$Mn^{3+}SOD(H_2O) - O_2^{2-} (+ H^+) \rightarrow Mn^{3+}SOD(OH^-) + H_2O_2 \quad (9)$$

2.3 Iron superoxide dismutase (FeSOD)

FeSOD was first discovered in prokaryotes, of which the structure is similar to that of MnSOD. As shown in Fig. 6, FeSOD is a dimer and each monomer has an iron-centered active site that contains a single iron binding three histidines, an aspartic acid and a water molecule. Although the active sites of FeSOD and MnSOD are similar in structure, the substitution of their metal ions with each other results in reduced activity.[37] The overall catalytic mechanism of FeSOD also relies on the conversion between Fe^{2+} and Fe^{3+} in a ping-pong manner.[24,37]

2.4 Nickel superoxide dismutase (NiSOD)

NiSOD was discovered in recent years. The structure of NiSOD is a homohexamer, with a Ni binding hook formed by the combination of Ni and some amino acid residues in the center of each monomer (Fig. 7). Unlike other SODs, in addition to histidine and aspartic acid, NiSOD has a large number of cysteine residues linked to the active center Ni *via* S–Ni bonds. However, the metal-bound cysteines are highly oxidation-sensitive and susceptible to damage. Studies have shown that all Ni related redox enzymes contain cysteine or redox non-harmless ligands. How NiSOD avoids the oxidative damage of S–Ni bonds and the catalytic mechanism of NiSOD are still being explored. However, it is certain that the mechanism of catalytic disproportionation is related to the transformation between Ni^{2+} and Ni^{3+}.[38]

In summary, this section briefly introduces the active center of natural SODs and their catalytic mechanism. The active centers of the above four common natural SODs have similar structures, that is, usually containing histidine and metal ions that are always coordinated with the nitrogen in the amino acid residues in the catalytic microenvironment. Besides, these natural SODs all have their own unique structures, which are mainly reflected in the use of hydrogen bond network, hydrophobic, and electric charge interactions, coordination with special amino acids and so on. These special structures make natural enzymes different in their substrate affinity, proton transfer efficiency, and redox reactivity, which ultimately lead to their different catalytic efficiencies. We hope that the summary of the structure and mechanism of natural SOD enzymes can provide references and inspirations for future research, so that SOD-like nanozymes will more closely simulate the natural enzymes, so as to exhibit a more potent catalytic performance.

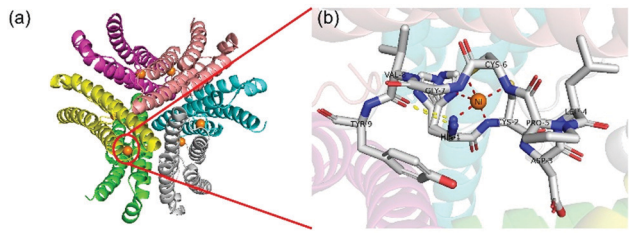

Fig. 7 Schematic illustration of NiSOD. (a) The structure and (b) active sites of *Streptomyces coelicolor* NiSOD (pdb ref: 1t6u). Picture created with PyMOL.

3. The development and mechanism of SOD nanozymes

On the basis of the research on the structure and mechanism of natural SODs, various types of nanozymes have been gradually developed.

3.1 Classification of SOD-like nanozymes

In 1985, Kroto *et al.* reported that C_{60} exhibited superoxide radical scavenging activity, which is an early proof that materials may simulate SOD-like activity, but the concept of nanozymes had not yet been proposed.[39] Since then, various SOD-like nanomaterials have been gradually developed. Up to now, about 100 kinds of nanozymes have been found to exhibit SOD-like activity, most of which consist of transition metals (*e.g.* Fe, Co, *etc.*) and elements such as carbon, nitrogen, oxygen, sulfur, *etc.* The following is a brief introduction of the most-studied nanozymes with SOD-like activity and their catalytic mechanism.

3.1.1 SOD-Like activity of cerium oxide nanoparticles. Cerium oxide nanoparticles are currently the most commonly used nanozyme with SOD-like activity due to their high biocompatibility and low toxicity. The SOD-like activity of cerium oxide nanoparticles was first reported by Korsvik *et al.* in 2007.[10] The SOD-like activity of cerium oxide nanoparticles is mainly related to the transformation between Ce^{3+} and Ce^{4+}. Due to the change of the valence of cerium oxide, cerium oxide forms oxygen vacancies or defects in the lattice structure by losing oxygen and electrons. These oxygen vacancies are the key structural features for cerium oxide nanoparticles to exert SOD-like activity. This rapid formation and disappearance of oxygen vacancies provide the ability to store and release oxygen. The oxygen vacancies cause the cerium oxide to release oxygen on the surface and stabilize the formation of linear oxygen vacancy clusters, which are the main defect structures on strongly reduced surfaces.[40] The size of nanoparticles has a great influence on the SOD-like activity of cerium oxide nanoparticles. On the one hand, the reduction of the size increases the specific surface area; on the other hand, the reduction of the size exposes more oxygen vacancies on the surface of cerium oxide nanoparticles.[10] In addition, the Ce^{3+}/Ce^{4+} ratio on the material surface also affects

the enzyme-like activity of cerium oxide nanoparticles, which may be related to the structure of oxygen vacancy. Each oxygen vacancy center is a Ce^{3+} surrounded by Ce^{4+}, so increasing the ratio of Ce^{3+} also increases the vacancy abundance, thus increasing the SOD-like activity.[41]

The synthesis methods of cerium oxide nanozymes include the oxidation of $Ce(NO_3)_3{\cdot}6H_2O$ with an oxidizing agent, such as hydrogen peroxide, ammonium hydroxide or NaOH.[42–44] Another method is to induce a reaction between $(NH_4)_2Ce(NO_3)_6$ and CH_3COONa.[45]

3.1.2 The SOD-like activity of carbon materials: fullerenes. Fullerenes are the first reported materials to exhibit SOD-like activity.[39] Fullerene has been called as free radical sponge because of its unique chemical reaction with free radicals. To solve the issue of the insolubility of fullerene, Dugan *et al.* modified fullerene with hydroxyl to enhance its solubility. They found that the modified fullerene still maintained the SOD-like activity.[46] Another study by them on C_{60}–C_3 materials showed that the SOD-like activity of fullerene was caused by superoxide dismutation, rather than stoichiometric scavenging. The C_{60}–C_3 surface electron defect regions promote the adsorption of $O_2^{\bullet-}$ and dismutate them with the help of protons from carboxyl groups and water molecules. They also found that the molecular symmetry of the material helped to increase the SOD-like activity, which is related to the polarity of the material. The specific catalytic mechanism is shown in Fig. 8(a).[4] In addition, the SOD-like activity of this material is also related to the number of carboxyl groups on fullerenes.[47]

Fullerenes used in studies are mostly obtained through purchase and are usually modified by various chemical methods. The synthesis of other carbon materials involves more diverse and complex chemical reactions and involves more steps. For example, in a study a pyrolysis method was used to mix melamine and formalin/phenol together using a Pluronic F127 soft template as the nitrogen and carbon sources, respectively, to prepare N-doped porous carbon nanospheres.[48] In another study, aniline and colloidal silica were mixed together, then the aniline was polymerized and carbonized, and the silica was removed to synthesize N-doped sponge-like carbon spheres.[49]

3.1.3 Other nanozymes with SOD-like activity. Some other metals such as Pt,[50] Au,[51] Cu,[52] Mn,[53] Ni,[54] Co,[55] Mo,[56] Rh,[57] Fe,[22] and V[58] and their oxides, carbides, nitrides and sulfides were also found to exhibit SOD-like activity. The main mechanism of their SOD-like activity includes the protonation of $O_2^{\bullet-}$ and the adsorption and rearrangement of $HO_2^{\bullet}$ on the metal surface. An investigation of the SOD-like activity mechanism of various metal nanoparticles showed that $O_2^{\bullet-}$ can easily capture protons in water to form $HO_2^{\bullet}$ and OH^-. $HO_2^{\bullet}$ adsorption on the surface of Au, Ag, Pd and Pt is a highly exothermic process that is likely to occur. As shown in Fig. 8(b) and (c), $HO_2^{\bullet}$ has very low potential energy profiles for rearrangement on Au and Pt surfaces. This means that, once $HO_2^{\bullet}$ is adsorbed on the surface, it can easily convert to O_2* and H_2O_2*. After that, O_2* and H_2O_2* turn into O_2 and H_2O_2.[5]

At the same time, some materials composed of two or more metals such as Au and Pt or Fe and Cu,[59,60] some polymers such as PLGA,[61] PEG,[62] and hydrogels[63] and materials with different shapes such as graphitic carbon nitride nanosheets[43] and NiO nanoflowers[54] have been developed. However, the current research on the catalytic mechanism is not in-depth. Several new methods for exploring the mechanisms are being developed. For example, density functional theory (DFT) and microkinetic modeling are used to determine the reaction route. The team of

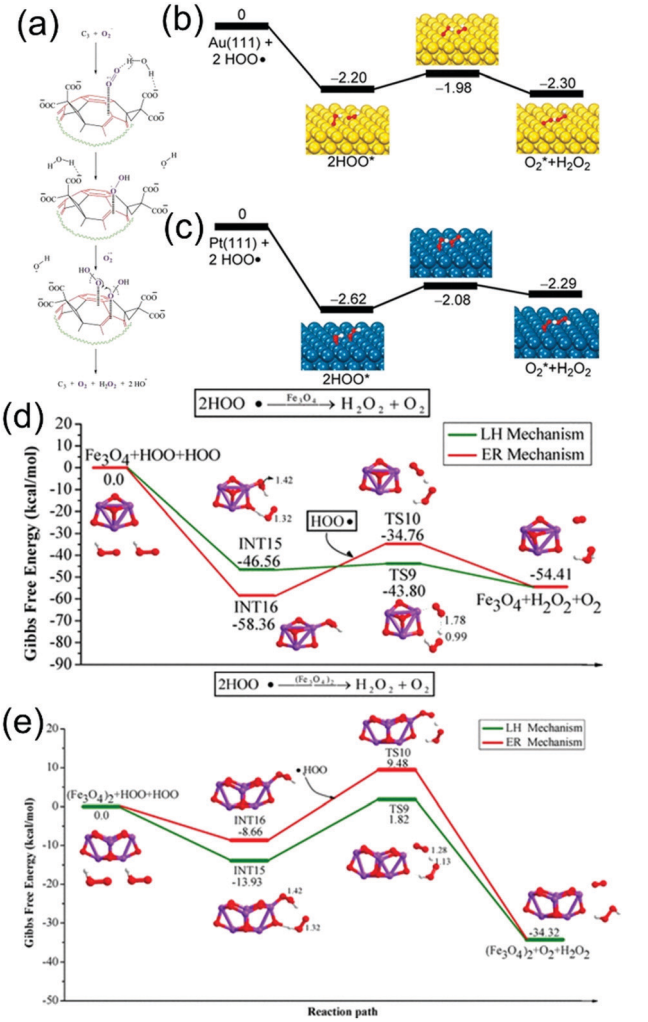

Fig. 8 Different kinds of nanozymes and their mechanism exploration. (a) Schematic representation of the catalytic interaction of C_3 and $O_2^{\bullet-}$. Chemical bonds colored in red are associated with electron-deficient areas. The incoming superoxide ions and the oxygen atoms derived from them are colored in purple. Broken lines represent the hydrogen bonding between oxygen and hydrogen atoms and hyphenated lines are used to represent the electrostatic attraction between negatively charged oxygen atoms and electron-deficient areas on the C_{60} moiety. In the proposed mechanism, C_3 is suggested to electrostatically drive superoxide anions toward electron-deficient areas on its surface until a second $O_2^{\bullet-}$ arrives to undergo dismutation with the help of protons from carboxyl groups and/or surrounding water molecules.[4] Reproduced with permission. Copyright 2004, Elsevier. (b and c) Potential energy profiles for rearrangements of two $HO_2^{\bullet}$ groups on the (111) facets of (b) Au and (c) Pt.[5] Reproduced with permission. Copyright 2015, American Chemical Society. (d and e) Calculated reaction energy profiles corresponding to the SOD-like activity of (d) Fe_3O_4 and (e) $(Fe_3O_4)_2$.[14] Reproduced with permission. Copyright 2019, American Chemical Society.

Guo used this method to evaluate whether the catalytic mechanism of a range of nanomaterials resembles Langmuir–Hinshelwood (LH) or Eley–Rideal (ER) processes.[14] Taking $(Fe_3O_4)_n$ as an example, they listed various intermediate transition states in two reaction routes, LH and ER, respectively, and calculated the reaction energy profiles of the reaction generated in each transition state (Fig. 8(d) and (e)). Then, they evaluated the heat release of the potential energy surface of the two mechanisms and finally proved that both Fe_3O_4 and $(Fe_3O_4)_2$ reacted through the LH route. In addition, they also evaluated a series of kinetic parameters in the reaction process by means of microkinetic modeling, which further proved that both Fe_3O_4 and $(Fe_3O_4)_2$ reacted through the LH pathway.[14] In a similar way, their team also evaluated the SOD mechanism of $(Co_3O_4)_n$ nanozymes and $Co_nFe_{3-n}O_4$ (n = 1–2) nanozymes. The results showed that, unlike $(Fe_3O_4)_n$, $(Co_3O_4)_n$ was catalyzed through the ER pathway and that $CoFe_2O_4$ exhibited a better SOD-like activity than Co_2FeO_4.[64,65]

There are many metal nanozymes, and their synthesis methods are also diversified. Some metallic elemental nanoparticles are usually prepared by reduction methods. For example, in a study, ethanol was used as the reducing agent to prepare nano-Pt by reducing H_2PtCl_6, and PVP as the protective reagent to control the size of Pt nanoparticles.[50] Some metal oxides are usually prepared by the oxidation or reduction of metal-containing salts. For example, in a study Co_3O_4 was formed through the oxidation of Co $(NO_3)_2{\cdot}6H_2O$ by ammonia and hydrogen peroxide.[55] In another study, Mn_3O_4 was prepared by adding oleic acid into $KMnO_4$ and then calcining the mixture in air.[66] The hydrothermal method is also used in the synthesis of Mn_3O_4 by adding $Mn(OAc)_2{\cdot}4H_2O$ and anhydrous ethanol together.[67]

3.2 The regulation of the SOD-like activity of nanozymes

There are many factors affecting the SOD-like activity of nanozymes, including the physical and chemical properties of nanomaterials such as size, shape, composition, external modification of nanomaterials, and different reaction systems. This section briefly describes the factors and regulation methods of SOD-like activity.

3.2.1 Size and morphology. The relative specific surface area is an important factor affecting nanozyme activity, which is closely related to the size and morphology of nanomaterials. Nanozymes with a larger specific surface area expose more active sites on the surface, thus tending to exhibit a more significant catalytic activity. Baldim *et al.* measured the SOD-like activity of cerium oxide nanoparticles with different particle sizes and found that the SOD-like activity was almost inversely proportional to the particle size of cerium oxide nanoparticles (Fig. 9(a)).[9] Yang *et al.* measured the SOD-like activity of cerium oxide nanoparticles with different shapes. They found that, at the same ceria concentration, the SOD-like activity of ceria nanochains (CNHs) was the strongest, followed by ceria nanoclusters (CNLs) and finally ceria nanoparticles (CNPs) (Fig. 9(b)). The differences in SOD-like activity were attributed to the different specific surface areas among the samples.[11] Similarly, the SOD-like activity of Mn_3O_4 nanoparticles with different shapes was also measured. The SOD-like activity of flower and flake structures was much higher than that of cubes, polyhedrons and hexagonal plates (Fig. 9(c)) because the nanoflower structure contains larger pores as active site pockets similar to natural enzymes.[12]

3.2.2 The quantity and valence of the active site. Although the relative specific surface area has a great influence on the enzyme-like activity of nanozymes, it is not the only factor. Studies have shown that the SOD-like activity of cerium oxide nanozyme was closely related to Ce^{3+}/Ce^{4+}, and the Ce^{3+} part plays a dominant role in the SOD catalytic process of cerium oxide nanoparticles.[68] In a study, He *et al.* proved this point in more detail. They synthesized two cerium oxide nanoparticles by different methods and heated for 15 min, 2 h and 8 h during synthesis. They found that, although the particle size of cerium oxide nanoparticles synthesized by microwave irradiation (CNPs-M) is only slightly larger than that of cerium oxide nanoparticles synthesized by convective heating (CNPs-C), the SOD-like activity of the former is much higher than that of the latter. The Ce^{3+}/Ce^{4+} ratio of each material was measured by an X-ray photoelectron spectroscopy (XPS) experiment. The results showed that the Ce^{3+}/Ce^{4+} ratio of CNPs-C was slightly higher at a heating time of 15 min, while it was lower at 2 h and 5 h, which was not completely consistent with their ROS scavenging efficiency (Fig. 9(d) and (e)), suggesting that the key factor of the SOD-like activity of cerium oxide nanoparticles was not the total Ce^{3+} concentration, but the surface Ce^{3+} concentration of the material. Then, they further verified the level of Ce^{3+} on the surface of the cerium oxide nanoparticles by oxidizing the surface with a strong oxidant. The absorbance change was measured to determine the amount of Ce^{3+} on the surface. It was found that the absorbance of oxidized CNPS-M changed greatly, proving that the surface contained more Ce^{3+} after oxidation (Fig. 9(f)).[13] In addition to cerium oxide nanoparticles, a study on manganese oxide nanoparticles showed that the SOD-like activity of Mn^{2+} and Mn^{3+} valence mixed Mn_3O_4 was much higher than that of MnO_2 with single valence because the circulation and conversion of oxidized Mn^{3+} and reduced Mn^{2+} are very important to the SOD-like activity.[12]

3.2.3 Cladding and modification. In addition to the nature of the material itself, other additional components of the material may also affect the SOD-like activity of nanozymes. San *et al.* coated PtNPs in the same crystalline states with PepA, DegP, and ClpP proteins, respectively, and found that different proteins exhibited different effects on the SOD-like activity of nanoparticles. As shown in Fig. 9(g), PepA-PtNPs exhibited the highest SOD-like activity, followed by ClpP-PtNPs, and it was much lower for DegP-PtNPs, which was not inversely proportional to the size of the nanoparticles. Further investigation revealed that the coated protein possessed a solvent channel in the middle affecting the access of substrates to the catalytic surface. The channel of DegP was relatively narrow, so their activity was the lowest. The physical and chemical properties and the inner shape of the protein shell also affected the SOD-like activity to some extent, but the chemical interaction between the protein and nanoparticles was not well understood.[17] In addition, some coating materials such as PEG protected the cerium oxide from deactivation

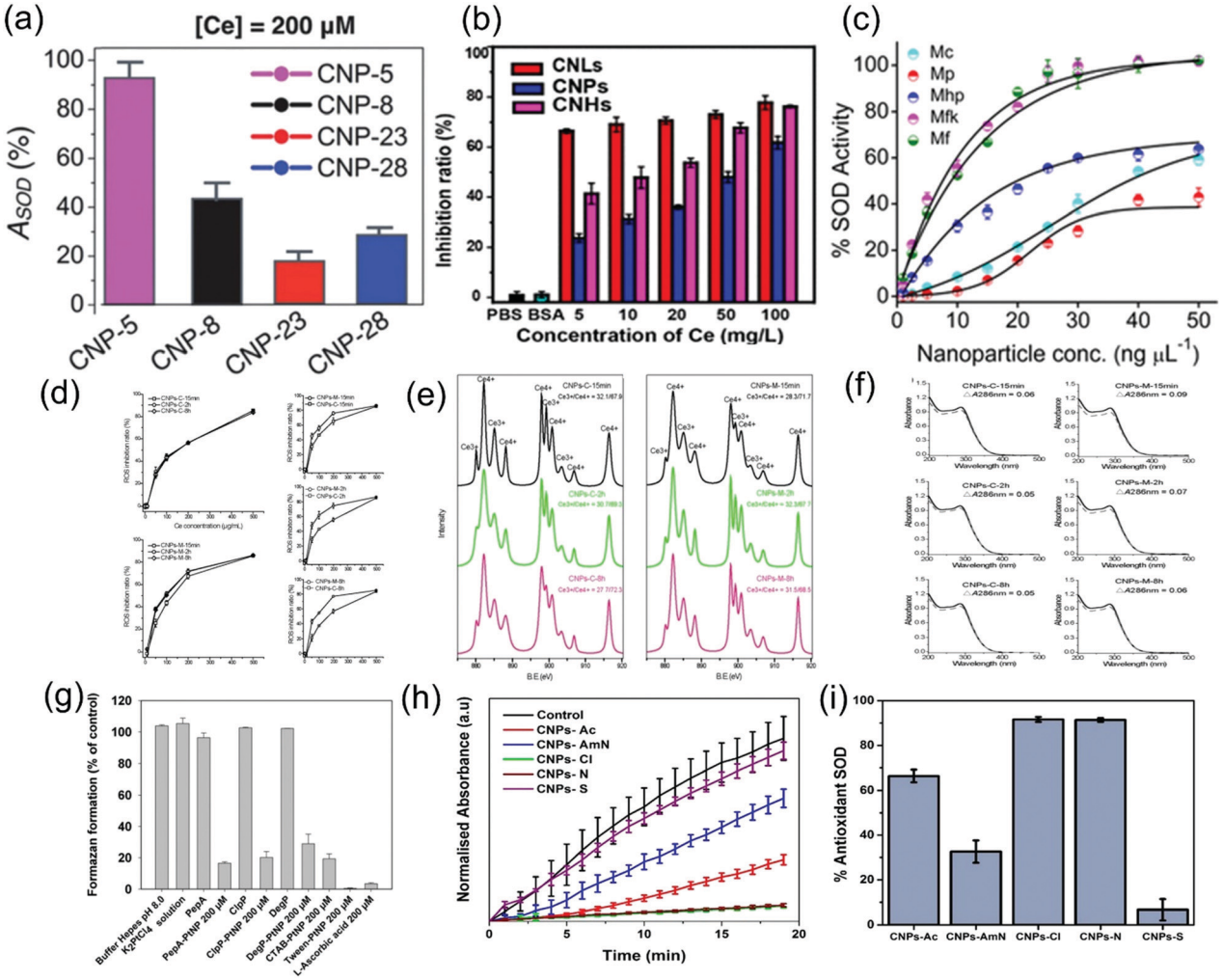

Fig. 9 Effects of different regulation methods on the SOD activity of nanozymes. (a) Effect of size on the enzyme activity of cerium oxide nanoparticles with sizes of 4.5 nm, 7.8 nm, 23 nm, and 28 nm.[9] Reproduced with permission. Copyright 2009, The Royal Society of Chemistry. (b) Effect of morphology on the enzyme activity of ceria nanochains (CNHs), ceria nanoclusters (CNLs) and ceria nanoparticles (CNPs).[11] Reproduced with permission. Copyright 2017, American Chemical Society. (c) Effect of morphology on the enzyme activity of Mn_3O_4 nano-cubes, nano-polyhedrons, nano-hexagonal plates, nanoflakes and nanoflowers.[12] Reproduced with permission. Copyright 2018, John Wiley and Sons. (d) ROS scavenging efficiency of CNPS-M and CNPS-C. (e) The Ce^{3+}/Ce^{4+} ratio of the material was characterized by XPS. (f) The change of absorbance before and after oxidation.[13] Reproduced with permission. Copyright 2017, Elsevier. (g) Effects of different coated proteins on the superoxide anion quenching ability and the SOD-like activity of PtNPs.[17] Reproduced with permission. Copyright 1991, The Royal Society of Chemistry. (h) SOD-like activity of CNPs synthesized using different precursors, cerium(III) acetate (CNPs-Ac), cerium(IV) ammonium nitrate (CNPs-AmN), cerium(III) chloride (CNPs-Cl), cerium(III) nitrate (CNPs-N), and cerium(III) sulfate (CNPs-S). Absorbance of WST-1 formazan dye at 440 nm in a 96-well plate plotted against the time course of the reaction. (i) The percent of antioxidant capacity of CNPs correlates with the SOD-like activity of CNPs.[18] Reproduced with permission. Copyright 2017, American Chemical Society.

by forming cerium phosphate in phosphoric acid.[25] However, PEG did not affect the SOD-like activity under normal conditions.[69] There are also some materials such as Au-core CeO_2-shell NP-based nanozyme that may be inactivated by cladding such as mercaptoundecanoic acid (11-MUA).[70]

Besides the cladding component, some modified components also affect the SOD-like activity of nanozymes. A study modified cerium oxide nanoparticles with different anions of the precursor salt counterions. The results in Fig. 9(h) and (i) showed that cerium(III) nitrate (CNPs-N) and cerium(III) chloride (CNPs-Cl) exhibited a higher SOD-like activity, followed by cerium(III) acetate (CNPs-Ac), while cerium(III) sulfate (CNPs-S) and cerium(IV) ammonium nitrate (CNPs-AmN) did not show significant SOD-like activity because of their low dispersion stability. The surface of CNPS-N presents more Ce^{3+}, resulting in a higher SOD-like activity. Although the Ce^{3+} concentration on the surface of CNPS-Cl is low, the presence of Cl^- changes the catalytic antioxidant performance of CNPS-Cl because it indirectly alters the surface chemistry, which decreases the oxidation potential. The transformation of Ce^{3+} to Ce^{4+} is more likely to occur in the presence of Cl^- ions, thus improving SOD-like activity.[18] In addition, studies have shown that silicon dioxide NPs modified by imidazole, carboxyl and phenol exhibited SOD-like activity.[71] Modification of cerium oxide nanoparticles with some

ligands such as triethyl phosphite (TEP) mediated redox reactions and regulated SOD-like activity by increasing the ratio of Ce^{3+} and Ce^{4+} on the material surface.[72]

3.2.4 Biologically relevant conditions and environments. The pH of the system regulates the enzyme activity of nanomaterials. It has been reported that the removal of $O_2^{\bullet-}$ by PtNPs is carried out under neutral and alkaline conditions, but the activity is negligible under acidic conditions.[73] Phosphate may significantly reduce the SOD-like activity of cerium oxide nanoparticles by forming cerium phosphate with Ce^{3+}.[74] In addition, adding enzyme inhibitors (*e.g.* 3-amino-1,2,4-triazole (3AT)) to the system inhibits the activity of the Pt-apoferritin (Pt-apo) nanozyme.[75]

In summary, a series of SOD-like nanozymes have been developed on the basis of the natural enzyme elements and the mechanism of active sites. In addition, the activity mechanism and regulation mode of these SOD-like nanozymes have been gradually explored. However, the research on the mechanism of SOD-like nanozymes is still relatively shallow. Some new exploratory techniques and methods also urgently need to be developed. We hope that the summary of this section can inspire further mechanism research, so as to develop SOD-like nanozymes with a higher activity, more explicit active sites and a better coordination between the active sites and framework structure.

4. Methods for measuring the SOD-like activity of nanozymes

Compared with peroxidase, oxidase and catalase, the characterization method for the SOD-like activity of nanozymes was not standardized yet. At present, the method for measuring the SOD-like activity of nanozymes is limited to qualitatively comparing the activities between nanozymes, and there are few quantitative studies on the specific activity and kinetic parameters. In fact, compared with the other enzyme activities that can be directly measured, the determination of SOD is relatively difficult. This may be due to the fact that the catalytic substrate of SOD, $O_2^{\bullet-}$, is a transient product and extremely unstable. Thus, the SOD-like activity is mostly determined by an indirect method. This section summarizes the current commonly used methods for the determination of SOD-like activity, hoping to provide some references for the development of more suitable methods for the determination of SOD-like activity in the future.

At present, most of the commonly used methods for the determination of the SOD-like activity of nanozymes are modified from the natural SOD activity assays. The key reagents in these methods are usually composed of two parts: the first part is used to produce $O_2^{\bullet-}$ and the second part is used to detect $O_2^{\bullet-}$. In most cases the principle is as follows. First, $O_2^{\bullet-}$ are generated through the first part of the reagent. These $O_2^{\bullet-}$ cause color or fluorescence changes in detection reagents such as chromogenic agents, and the amount of total $O_2^{\bullet-}$ produced in the system can be detected by these changes. When the nanozyme with SOD-like activity is added to the detection system, the production of $O_2^{\bullet-}$ is reduced, thereby inhibiting the changes in the detection reagent. By comparing the color/fluorescence change of the detection reagent before and after adding the nanozyme, the SOD-like activity of the nanozyme can be calculated.

The first method used to measure the SOD-like activity of the nanozyme was the detection system containing hypoxanthine, xanthine oxidase and cytochrome *c*. This method was first proposed by Korsvik *et al.* to detect the SOD-like activity of two different cerium oxide nanoparticles at different concentrations.[10] Singh *et al.* also used this method to determine the SOD-like activity of cerium oxide nanoparticles at different pH values.[74] Briefly, the mechanism is that xanthine oxidase catalyzes the hypoxanthine to produce $O_2^{\bullet-}$, and then $O_2^{\bullet-}$ oxidizes cytochrome *c*, resulting in the production of reduced cytochrome *c* with ultraviolet absorption at 550 nm. When a SOD-like nanozyme is added, it competes with cytochrome *c* for $O_2^{\bullet-}$, thus inhibiting the reduction of cytochrome *c* and reducing the change of absorbance. By measuring the changes of absorbance at 550 nm before and after nanozyme addition within a certain period of time, the SOD-like activity of different types and concentrations of material were determined. Using this method, the SOD-like activity of cerium oxide nanoparticles at different concentrations was compared (Fig. 10(a) and (b)). In some cases, excess catalase is added to the system to remove the product H_2O_2. Xanthine is also used in some methods instead of hypoxanthine.[76]

Except for using xanthine and xanthine oxidase, there are other methods for $O_2^{\bullet-}$ production. Examples include the use of riboflavin under light illumination,[11] riboflavin and methionine,[77] and the direct production of $O_2^{\bullet-}$ [78] from KO_2, which is rarely used due to its extreme instability and toxicity.

With the development of the above methods, cytochrome *c* was found to be not sensitive and stable enough, and some other colorimetric reagents were used to replace cytochrome *c*, such as nitro blue tetrazolium (NBT),[25] water soluble tetrazolium salts (WST),[9] *etc.* Using these methods, a number of kits for the determination of SOD-like activity have also been developed.[79] In addition to colorimetric reagents, some other reagents have been used to detect $O_2^{\bullet-}$, such as lucigenin, which is detected by chemiluminescence,[80] and hydroethidine, an $O_2^{\bullet-}$ fluorescent probe.[81] In addition, electron paramagnetic resonance (EPR) or electron spin resonance (ESR) is also used to detect the amount of $O_2^{\bullet-}$. The ESR spectrum in Fig. 10(c) shows the enzyme activity of natural SODs and the PtRu nanozyme at different ratios of Pt and Ru.[16]

Some other methods are also used to measure SOD-like activity, and some reagents are able to change color while producing $O_2^{\bullet-}$, such as the pyrogallol autoxidation method. Pyrogallol produces $O_2^{\bullet-}$ by autoxidation under alkaline conditions and further produces colored products such as *o*-hydroxy-*o*-benzoquinone with an ultraviolet absorption peak at 325 nm. In the presence of SOD, the colored products formed by pyrogallol reacting with $O_2^{\bullet-}$ are inhibited, and the SOD-like activity is determined by the inhibition rate.[82] By controlling the presence of FePOs and the presence of pyrogallol, it is proved that the autoxidation of pyrogallol is able to measure the SOD-like activity of FePOs (Fig. 10(d) and (e)).[22] Similarly, the epinephrine autoxidation method uses epinephrine

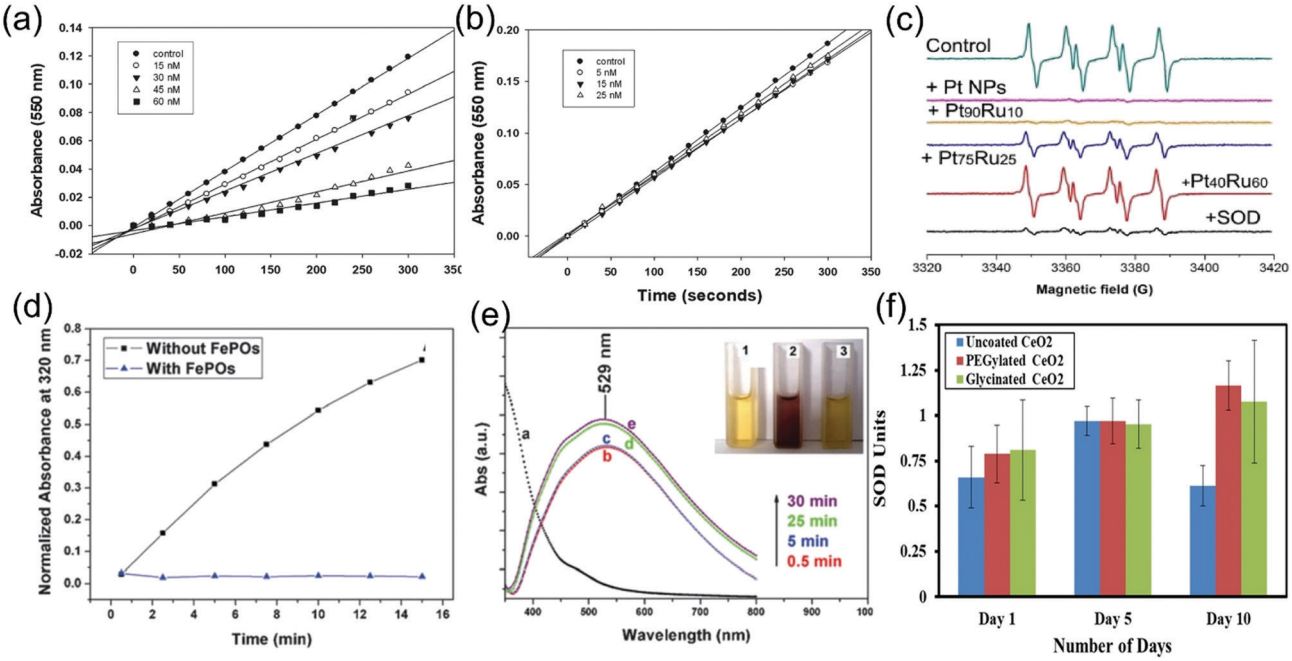

Fig. 10 Different methods to characterize the SOD activity of nanozymes. (a and b) The SOD-like activity of two different cerium oxide nanoparticles with different Ce^{3+}/Ce^{4+} ratios at different concentrations determined using hypoxanthine, xanthine oxidase and cytochrome *c* system.[10] Reproduced with permission. Copyright 1996, The Royal Society of Chemistry. (c) ESR spectra of BMPO/•OOH generated from the control sample, PtRu NP nanozyme at different ratios of Pt and Ru, and natural SOD-like enzyme.[16] Reproduced with permission. Copyright 2009, The Royal Society of Chemistry. (d) FePOs had inhibitory effects on the autoxidation of pyrogallol. (e) The degree of autoxidation of pyrogallol changed with time: (1) only FePOs microflowers; (2) FePOs microflowers and pyrogallol; and (3) only pyrogallol.[22] Reproduced with permission. Copyright 1996, The Royal Society of Chemistry. (f) The SOD-like activity of CeO_2 nanoparticles in various layer materials represented by a specific activity: U.[25] Reproduced with permission. Copyright 2019, American Chemical Society.

autoxidation to produce $O_2^{\bullet-}$ and then produces adrenochrome with an ultraviolet absorption peak at 480 nm, which is inhibited in the presence of SOD-like nanozymes.[83]

In addition to the qualitative comparison of the activity of nanozymes, there are also a few studies using specific activity and enzyme reaction kinetic parameters and other methods to quantify the SOD-like activity. For example, Damle *et al.* reported that, in the xanthine, xanthine oxidase and NBT systems, the production rate of $O_2^{\bullet-}$ was regulated by adjusting the concentration of xanthine oxidase to fix the absorbance change value at 550 nm of NBT to 0.025 per minute. SOD-like activity is detected as the percentage of absorbance increase inhibited at 550 nm, also known as the inhibition rate. The unit of enzyme activity is defined as the amount of enzyme that inhibits the change of NBT by 50% per minute, namely IC_{50}. The corresponding specific activity is measured by normalizing the amount of nanozyme. As shown in Fig. 10(f), they used this method to measure the SOD-like activity of cerium oxide nanoparticles in various layer materials.[25] Moreover, Dashtestani *et al.* used the pyrogallol autoxidation method to explore the kinetic parameters of enzyme reactions, such as IC_{50} and k_{cat}, of NACu-Cys, which consists of the Cu-Cys complex and nano-albumin (NA), through the Michaelis–Menten equation.[82]

Some common methods for the determination of SOD-like activity of nanozymes is shown in Table 2. In present, the SOD-like nanozyme activity determination method still faces some challenges. The most important one is that the enzyme activities of different materials in different studies could not be compared due to the inconsistency of the substrate and sensitivity of different determination methods. Liu *et al.* compared various determination methods and evaluated the advantages and disadvantages of each method. They used the xanthine/xanthine oxidase method and the irradiation of riboflavin method to produce $O_2^{\bullet-}$, and employed hydroethidine (HE), NBT, iodonitrotetrazolium chloride (INT), WST, cytochrome *c*, and 5,5-dimethyl-1-pyrroline-*N*-oxide (DMPO) (EPR) to detect $O_2^{\bullet-}$. Finally, they came to several conclusions: (1) the HE probe may be disturbed by the oxidizing nanozymes; (2) the NBT probe has limited sensitivity due to the poor water solubility of its products; (3) the sensitivity of WST is higher than those of NBT and INT; (4) the method of producing $O_2^{\bullet-}$ by riboflavin irradiation may be disturbed by the electron accepting ability of nanozymes; (5) EPR is sensitive and both the quality of DMPO and incubation time are important factors for the EPR measurement.[84] In addition, there is another problem that deserves attention. Most of the current measurement methods have been derived from the method of determination of natural SOD enzyme activity, which might not be very suitable for inorganic nanocomposites. Other components in the system may cause disturbance to the measured results, for example, various kinds of buffer may result in gathering or breakdown of the nanozyme, and the Ethylene Diamine Tetraacetic Acid (EDTA)

Table 2 Different methods for the determination of the SOD-like activity of nanozymes

Nanozymes	Reagent/enzyme activity determination methods	Representative methods	Ref.
C_{60}-PLGA	Hypoxanthine, xanthine oxidase enzyme, DMPO	EPR	85
C_{60}, C_{70}	Xanthine, xanthine oxidase, cytochrome *c*	IC_{50}	86
CeO_{2-x} NPs and $GdYVO_4$:Eu^{3+} NPs[a]	Epinephrine autoxidation	Inhibition ratio	87
Cerium oxide nanoparticles	SOD assay kit	UV absorbance	88
Mn-NPs	Riboflavin, methionine, NBT	Inhibition ratio	89
MnO NPs	Xanthine, xanthine oxidase, cytochrome *c*	Inhibition ratio, k_{SOD}	90
Cerium oxide	Hypoxanthine, xanthine oxidase, cytochrome *c*	UV absorbance; specific activity: U	91
Biogenic magnetic nanoparticles	Pyrogallol autoxidation	Specific activity: U	92
Mn-MPSA-PCC[a]	KO_2	Cyclic voltammetry	93
MnO_x	Xanthine, xanthine oxidase, BMPO	ESR	94
Gd@C_{82}	Xanthine, xanthine oxidase, lucigenin	Chemiluminescence	95
CuTA	Xanthine, xanthine oxidase, INT	UV absorbance	96
Ce-MGBs[a]	WST assay kit	UV absorbance	97
NiO nanoflowers	Pyrogallol autoxidation; KO_2	UV absorbance; IC_{50}	54

[a] $GdYVO_4$:Eu^{3+} NPs: $Gd_{(0.7)}Y_{(0.2)}Eu_{(0.1)}VO_4$; Mn-MPSA-PCC: melamine-phytic acid-super molecule-aggregation modified on the surface of PCC through the assembly of amino groups, phosphate groups and oxygen-containing groups on PCC; Ce-MGBs: mesoporous bioactive glasses (MBGs) modified with cerium ions.

in the system may complex the metal ion components which determines the SOD-like activity, and so on. Therefore, better assay methods for detecting the SOD-like activity of nanozymes need to be established.

5. Antioxidant applications of SOD-like nanozymes

5.1 As antioxidants to protect cells

Utilizing the ROS scavenging ability, SOD-like nanozymes have been widely used to reduce the oxidative stress of the cell. For example, Bhushan *et al.* delivered cerium oxide nanoparticles into cells by coating with albumin, improving biocompatibility without reducing the antioxidant activity of cerium oxide nanoparticle nanozymes. Semi-quantitative RT-PCR analysis confirmed that albumin modified SOD-like nanozymes successfully defended against free radicals and alleviated oxidative damage to cells, while biocompatible albumin-encapsulated cerium oxide nanoparticles protected the antioxidant defense system of cells and protected cells from oxidative stress-mediated apoptosis.[45] Kamada *et al.* demonstrated that UV-induced DNA damage was inhibited by Ce-doped titanate nanosheets (CE-TNS).[98] It has also been found that cerium oxide nanoparticles eliminated ROS and prevented cell apoptosis by reducing the level of Caspase 3/7 and the loss of mitochondrial membrane potential. In addition to reducing ultraviolet A ray-induced fibroblast death, cerium oxide nanoparticles also promoted cell migration and proliferation.[99]

However, the use of SOD-like activity alone is not sufficient to eliminate all kinds of ROS. Therefore, nanozymes with the advantage of multi-enzyme activities are designed to further exert their antioxidant effects through cascade reactions. In the study of Singh *et al.*, a Mn_3O_4 nanozyme with the activities of catalase, glutathione peroxidase (GPx) and SOD was constructed. The multi-enzyme activities of these materials depend on many factors, such as morphology, specific surface area, pore size and redox properties. The cascade reactions could occur between these enzymatic activities (Fig. 11(a)). In detail, the Mn_3O_4 nanozyme captured $O_2^{\bullet-}$ and produced oxygen and H_2O_2 through SOD-like activity. Then, through catalase and GPx activities, the generated H_2O_2 was further converted into water and oxygen. As shown in Fig. 11(b) and (c), the Mn_3O_4 nanozyme greatly reduced the level of ROS in mitochondria and cells. Thus, SOD-like nanozymes provide significant protection against ROS mediated protein oxidation, lipid peroxidation and DNA damage.[8]

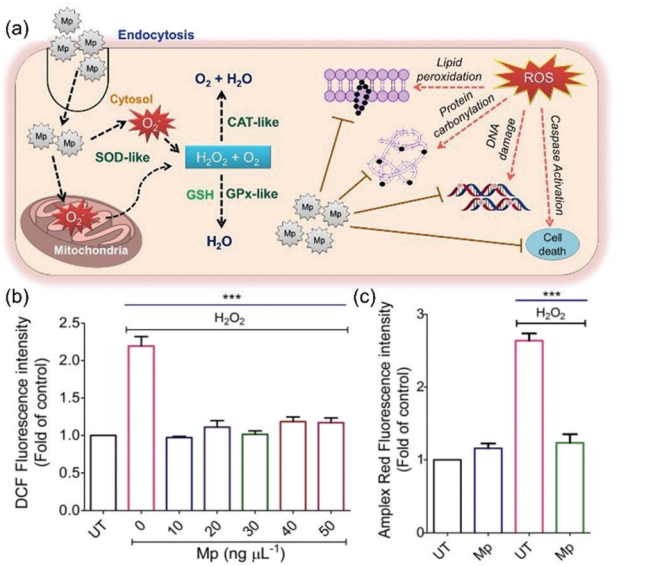

Fig. 11 Mn_3O_4 nanozyme exerted antioxidant effects in cells through cascading reactions. (a) Multi-enzyme mimetic Mn_3O_4 nanoflowers (Mp) modulated the redox state of mammalian cells without altering the cellular antioxidant machinery under oxidative stress conditions. (b and c) ROS scavenging activity of Mp was evaluated in mammalian cells. (b) Relative mean DCFDA fluorescence intensity of cells left untreated (UT) or pre-treated with variable concentrations of Mp prior to H_2O_2 treatment. (c) The H_2O_2 scavenging ability of Mp was confirmed using a H_2O_2 specific dye, Amplex Red.[8] Reproduced with permission. Copyright 2009, The Royal Society of Chemistry.

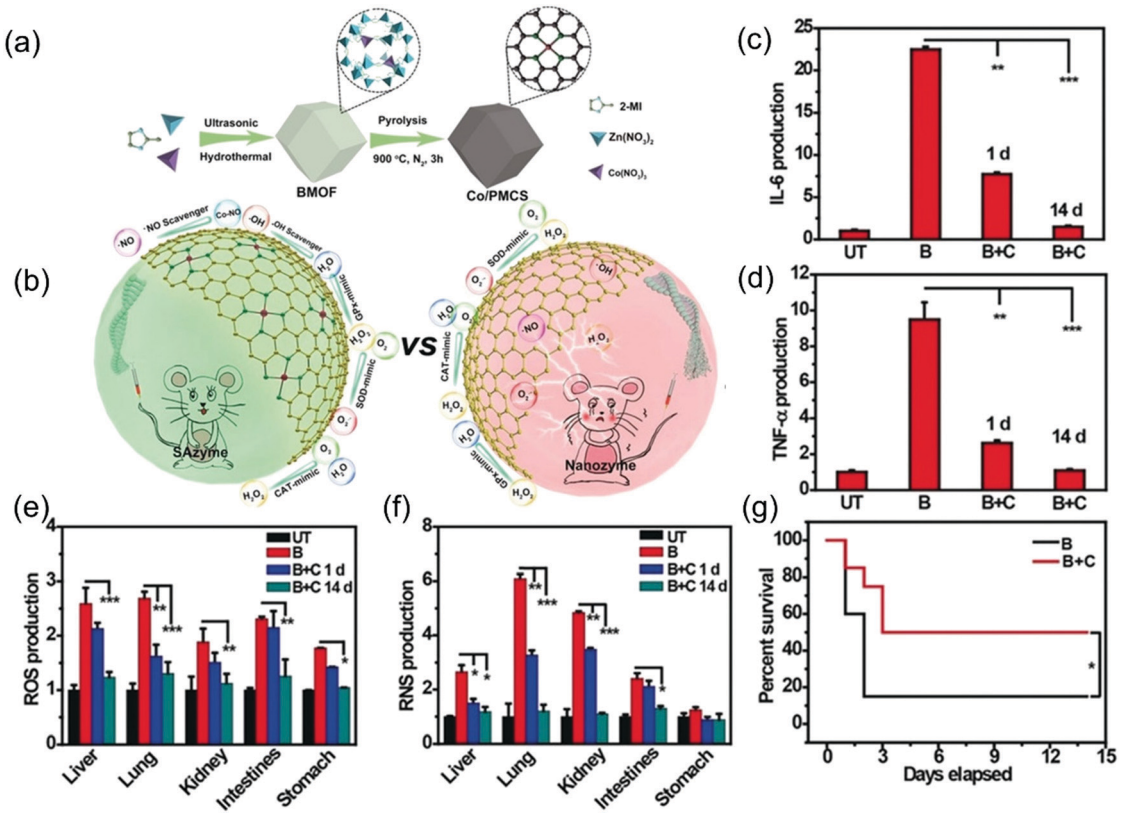

Fig. 12 Co/PMCS nanozyme was used to treat sepsis. (a) Illustration of the formation of Co/PMCS. (b) The use of multi-antioxidant SAzymes for sepsis management that defeats nanozymes. (c and d) Detection of (c) IL-6 and (d) TNF-α *in vivo* in different groups. (e and f) Determination of (e) ROS and (f) RNS *in vivo* in different tissues. UT: untreated, B: LPS, C: Co/PMCS. (g) Survival curves of the two groups observed for 14 days.[3] Reproduced with permission. Copyright 2020, John Wiley and Sons.

In all, SOD-like nanozymes have the ability to eliminate ROS and therefore protect cells from oxidative stress such as DNA damage, protein oxidation and lipid peroxidation. Through the cascade of SOD-like activity and other activities such as catalase and glutathione peroxidase, the antioxidant function of nanozymes could be further promoted.

5.2 Treatment of oxidative stress related diseases

5.2.1 Treatment of sepsis. The antioxidant function of SOD is also used to treat a series of antioxidant-related diseases, among which the most common one is inflammation-related diseases. Sepsis is a systemic inflammatory response syndrome caused by a local infection. Due to the lack of effective treatment, sepsis exhibits the characteristics of high morbidity and mortality. Excessive production of reactive oxygen and nitrogen species (RONS) due to inflammation plays a crucial role in the pathophysiology of sepsis. Cao *et al.* eliminated ROS through a catalase, GPx and SOD cascade reaction of a single Co atom nanozyme, which also magically eliminated •NO by coordinating Co-porphyrin centers (Fig. 12(a) and (b)). Proinflammatory factors such as TNF-α and IL-6 (Fig. 12(c) and (d)) and free radicals such as RNS and ROS (Fig. 12(e) and (f)) are all significantly decreased after treatment with the Co nanozyme, indicating the anti-inflammation and antioxidant ability of the Co SOD-like nanozyme. These therapeutic effects ultimately increased the survival rate of septic mice treated with the Co nanozyme (Fig. 12(g)).[3]

5.2.2 Treatment of Alzheimer's disease. Alzheimer's disease is a neuroinflammatory disease. Excessive continuous stimulation of ROS, inflammatory cytokines, and Aβ activates pro-inflammatory M1 microglia, ultimately leading to irreversible neuron loss. The SOD-like activity of nanozymes eliminates ROS, reduces inflammation and thus treats Alzheimer's disease. Ren *et al.* constructed the (3-carboxypropyl)triphenyl-phosphonium bromide functionalized molybdenum disulfide quantum dot (TPP-MoS_2 QD) nanozyme to treat Alzheimer's disease. This TPP-MoS_2 QDS nanozyme possesses the activities of catalase and SOD, which scavenged ROS and down-regulated various pro-inflammatory cytokines. With the help of TPP, the TPP-MoS_2 nanozyme successfully escaped from lysosomes and targeted mitochondria. In addition, the TPP-MoS_2 QD nanozyme stimulated the transition of microglia from inflammatory M1 phenotype to anti-inflammatory M2 phenotype, which degraded Aβ deposition, thus realizing the protection of neurons.[100] To precisely target the site of the lesion, some Aβ-targeting ligands, such as KLVFFAED (KD8), were also modified on the nanozyme such as N-MCNs to increase their accumulation in the Aβ deposition site (Fig. 13).[6] Since nanozymes possess multifunctional properties, including their enzymatic activity and potential to be used as nanocarriers. Thus, SOD-like nanozymes also acted as gene drug delivery systems, *e.g.* siSOX9 and retinoic

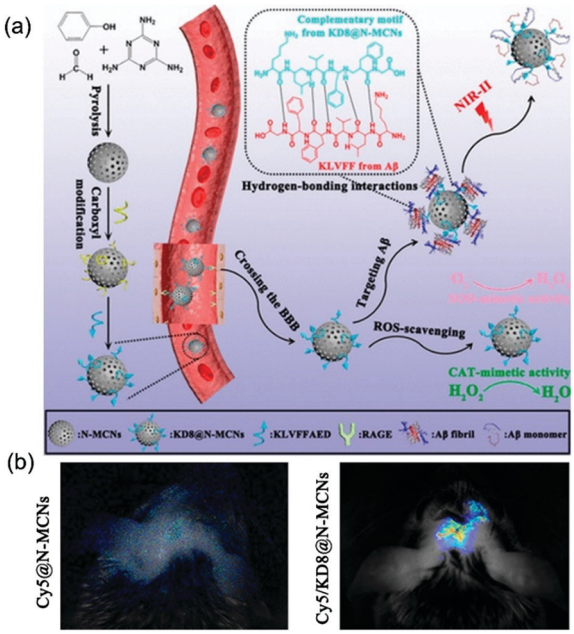

Fig. 13 KD8@N-MCNs nanozyme was used to treat Alzheimer's disease. (a) Schematic diagram of KD8@N-MCNs synthesis and the mechanism of action of KD8@N-MCNs. (b) *In vivo* imaging of 3xTg-AD mice administered with Cy5@N-MCNs or Cy5/KD8@N-MCNs.[6] Reproduced with permission. Copyright 2020, American Chemical Society.

acid (RA) co-delivered with ceria-doped MIL-100(Fe). siSOX9 down-regulated the expression of Sox9, thereby inhibiting gliogenesis, while RA up-regulated the expression of neuronal genes, which synergistically promotes the differentiation of neural stem cells like neuronal cells, thus treating Alzheimer's disease.[101] In conclusion, through modification and co-delivery methods, SOD nanozymes have a good prospect in the treatment of Alzheimer's disease.

5.2.3 Treatment of oral ulcers. Oral ulcers are often accompanied by the production of large amounts of ROS, which causes inflammation and accelerates the disease. Gu *et al.* modified VB_2 on iron oxide nanoparticles for the treatment of oral ulcers. VB_2 enhanced the SOD-like activity of iron oxide nanoparticles and facilitated iron oxide nanoparticles to remove ROS for cell protection. The iron oxide nanozyme also exhibited antibacterial activity against *Streptococcus mutans*, *Staphylococcus aureus* and *Escherichia coli*.[102]

5.2.4 Treatment of cardiovascular disease. Cardiovascular disease is a serious disease threatening human life. One of the most effective treatment strategies is the continuous administration of a mild, controlled supply of NO to protect the cardiovascular system from injury. Gold nanorods exhibit SOD-like and nitric oxide synthase (NOS) enzyme-mimic activity. Li *et al.* used gold nanorods to catalyze the oxidation of NADPH to produce $O_2^{\bullet-}$ and then to produce H_2O_2 through SOD-like activity, and finally H_2O_2 mediates the oxidation of arginine to produce NO, thus simulating the activity of nitric oxide synthase, which is used in the treatment of cardiovascular disease.[103]

5.2.5 Treatment of COVID-19. COVID-19 has been an unprecedented global health crisis since 2019. COVID-19 would lead to acute respiratory distress syndrome (ARDS), systemic inflammation, and finally serious pulmonary fibrosis. Therefore, it is an effective treatment approach to control the occurrence and development of inflammation by eliminating ROS. Prince *et al.* found that cerium oxide nanoparticles exhibited the antioxidant activity of SOD and catalase, and had the ability to inhibit NFκB, MAPKs and TGF-β signaling pathways, and therefore can be used to improve respiratory function during infection.[104]

5.2.6 Treatment of inflammation and injury. In the research conducted by Chen *et al.*, they delivered the CeO_2/Pt nanozyme into monolayer cross-linked zwitterionic vesicles (cZVs) to construct an artificial organelle (peroxisome) for the treatment of ear inflammation.[105] The SOD-like activity of nanozymes was also used to treat other antioxidation-related diseases, including enteritis,[106] lung injury,[96] psoriasis,[107] *etc.*

In all, SOD-like nanozymes are used in the treatment of a large series of antioxidant diseases such as sepsis, Alzheimer's disease and almost all kinds of inflammation based on their ability to eliminate ROS. SOD-like nanozymes would achieve a better therapeutic effect by coating, modifying or co-loading other drugs.

5.3 Other applications

In addition to the treatment of diseases, SOD-like nanozymes have been widely used in other fields. Li *et al.* developed a method for *in vivo* encapsulation of MnO_2 nanozyme shells on the surface of living yeast cells. The nanozyme shell not only enhanced the tolerance of cells to severe physical stressors, including dehydration and lyase, but also kept the cells alive after prolonged exposure to high levels of toxic chemicals. In addition, these coated cells were fully restored to growth and function by simple biomolecular stimulation to remove their shells. This strategy has the potential to be applied to a wide range of living cells.[108]

In the process of winemaking, with the accumulation of alcohol and changes in pH, temperature and osmotic pressure, yeast may produce a large amount of ROS, thus reducing the vitality and fermentation efficiency of yeast. Zhou *et al.* used FeCo-PBA NPs to scavenge ROS, thus greatly improving the tolerance of yeast to ethanol and reactive oxygen species, improving the metabolic activity of yeast, and increasing alcohol production.[81] ROS is an important cause of cell and organism senescence. Kim *et al.* constructed nano-Pt and treated nematodes. The results showed that nano-Pt significantly reduced the accumulation of lipofuscin and ROS induced by paraquat, and the lifespan of nematodes was significantly enhanced after treatment, proving that the Pt nanozyme has an anti-aging effect.[50] In addition, some nanozymes are also used as sperm cryopreserved protectants to combat the oxidative stress caused by ROS production during sperm cryopreservation, thus reducing apoptotic necrosis and enhancing the activity.[109] Some other applications such as the detection of $O_2^{\bullet-}$ also use the SOD-like activity of nanozymes.[110]

Although the SOD-like activity of nanozymes is mainly used for antioxidant therapy, due to the multi-enzyme activities of nanozymes, they sometimes also cascade with peroxidase

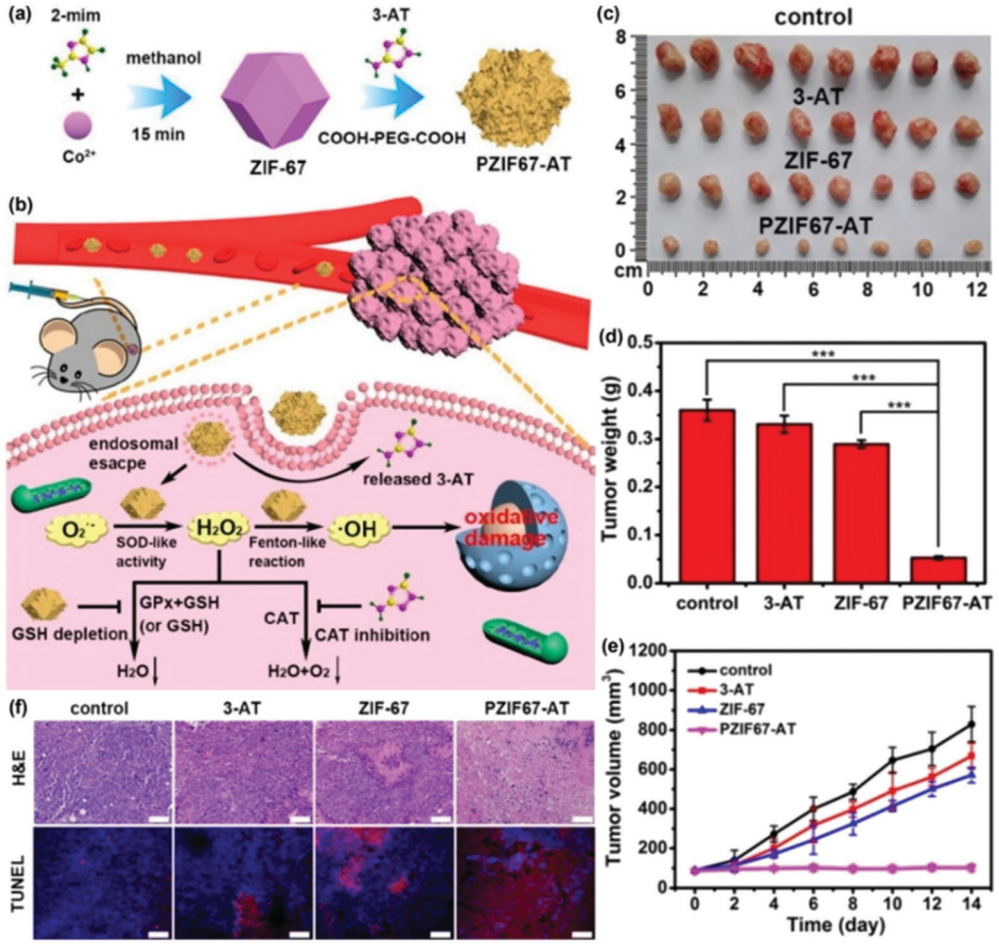

Fig. 14 Antitumor study of zeolitic imidazole framework-67 (ZIF-67) nanozyme as a H_2O_2 homeostasis disruptor for intensive chemodynamic therapy. (a) Preparation of PZIF-67-AT nanoparticles. (b) Intensive chemodynamic therapy induced by PZIF-67-AT nanoparticles. (c) Photographs of the dissected tumors treated with four samples for 14 days. (d) Weights of the tumors. (e) Changes in tumor volumes. (f) Tumor tissue staining by H&E and TUNEL.[7] Reproduced with permission. Copyright 2021, Elsevier.

activity or Fenton regents to promote the generation of hydroxyl free radicals, thereby being used to treat tumors by promoting oxidation. By modifying the small-molecule inhibitor 3-amino-1,2,4-triazole (3-AT) and PEG on zeolitic imidazole framework-67 (ZIF-67) nanoparticles, PZIF67-AT was prepared by Sang *et al.* (Fig. 14(a)). As shown in Fig. 14(b), the SOD-like activity of ZIF-67 was used to convert $O_2^{\bullet -}$ into H_2O_2, and then chemodynamic therapy (CDT) was used to convert H_2O_2 into more $^{\bullet}OH$ through Fenton reaction. In addition, ZIF-67 could also deplete glutathione to inhibit the conversion of H_2O_2 into a non-toxic form. Moreover, 3-AT inhibited the enzymatic activity of catalase, thus inhibiting the decomposition of H_2O_2. Based on this, the PZIF67-AT nanozyme enhanced the production of $^{\bullet}OH$ to destroy the tumor. After treatment with the PZIF67-AT nanozyme, the size, weight and volume of the tumor were significantly reduced (Fig. 14(c)–(e)). Moreover, the level of apoptosis in tumor tissues also increased after PZIF67-AT nanozyme treatment as shown by the TUNEL staining in Fig. 14(f).[111] In another way, as shown in Fig. 15, Kang *et al.* prepared speckled RuTe hollow nanorods (RuTeNRs) which exhibited the multiple activities of peroxidase/SOD/catalase. Through the

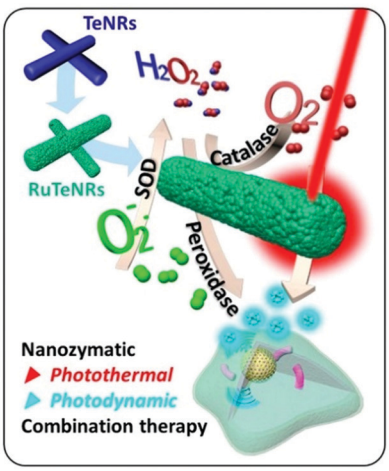

Fig. 15 Schematic illustration of RuTeNR synthesis and their nonrecurring circuit nanozymatic enhancement for hypoxic cancer phototherapeutic application.[2] Reproduced with permission. Copyright 2020, American Chemical Society.

Table 3 Applications of SOD-like nanozymes

Nanozyme (drugs used together)	Types of enzyme activity	Application/disease	Ref.
Pt@PCN222-Mn[a]	SOD/catalase	Inflammatory bowel disease	112
ZIF-67/$Cu_{0.76}Co_{2.24}O_4$ NSs[a]	Peroxidase/SOD/GPx/laccase-like activities	Real-time detection of living neurotransmitters	113
$Cu_{5.4}O$ USNPs[a]	SOD/catalase/GPx	Acute kidney/liver injury, wound healing	114
CeNPs (PTEN plasmid)	SOD	Prostate cancer	115
MnTPP/ERGO/GCE[a]	SOD	Real-time monitoring of $O_2^{\bullet-}$ from breast cancer cells	116
Single-atom Pt/CeO_2	SOD/catalase/peroxidase/GPx	Bandage for brain trauma and reducing neuroinflammation	117
CTMDs[a]	SOD/GPx-like	Alleviating endotoxemia	118
Cerium oxide nanoparticles	SOD	Restraining cerulein induced acute pancreatitis	119
MoO_{3-x} nanodots	Catalase/SOD	Treatment of amyloid induced neurotoxicity	120
Cu_xO nanoparticle clusters	Peroxidase/SOD/catalase/GPx	Ameliorating Parkinson's disease	121
PGNPNF[a]	SOD	Wound healing applications	122
Mn_3O_4 nanozymes	SOD/catalase	Protecting ear-inflammation	67
$FePO_4$	SOD	Real-time detection of $O_2^{\bullet-}$	123
Pt-NPs	SOD/catalase	Alleviating apoptosis	124
Pt NPs	SOD	Treating vascular diseases such as atherosclerosis	125

[a] Pt@PCN222-Mn: Mn(III)porphyrin and Pt NP within a nanoscale Zr-based MOF, PCN222; ZIF-67/$Cu_{0.76}Co_{2.24}O_4$ NSs: "raisin pudding"-type ZIF-67/$Cu_{0.76}Co_{2.24}O_4$ nanospheres; $Cu_{5.4}O$ USNPs: ultrasmall $Cu_{5.4}O$ nanoparticles; MnTPP/ERGO/GCE: manganese(III) tetraphenyl porphine/electrochemical reduced graphene oxide/glassy carbon electrode; CTMDs: Cu-TCPP MOF nanodots; PGNPNF: cerium oxide nanoparticle functionalised polycaprolactone (PCL)-gelatin nanofiber.

cascade of these activities, oxygen and ROS ($^{\bullet}OH$) were abundantly produced, which on the one hand alleviated the hypoxic environment of the tumor and on the other hand were combined with photodynamic and photothermal therapy to destroy the tumor.[2]

Table 3 gives some more examples of the application of SOD-like nanozymes. This covers almost all the applications of SOD-like nanozymes to date. We hope that the summary of various applications of SOD-like nanozymes can provide some inspiration for future research and applications. We also hope that SOD-like nanozymes can be applied to more and more suitable fields.

6. Conclusion and prospects

As a new generation of artificial enzymes, SOD-like nanozymes have great potential to replace natural SODs in removing ROS, protecting cells from oxidative damage, reducing tissue inflammation and anti-aging, and effectively solving the limitations of natural SODs.

In the development process of this field, the exploration of mechanism is the most important and difficult process. Therefore, this paper reviews the structure and activity mechanism of several natural SODs, in order to summarize the mechanism of SOD-like nanozymes and provide a direction for their design and regulation.

Due to the development of different kinds of nanozymes with high enzyme activity, methods for the characterization of enzyme activity have been gradually developed. At the same time, the abundant species and high enzyme activity make the application of SOD-like nanozymes gradually diversified. Based on their ability to remove $O_2^{\bullet-}$ in ROS, the SOD-like activity of nanozymes is mainly used in antioxidant therapy. Due to the unique multi-enzyme activity characteristics of nanozymes, the cascade of multi-enzyme activities helps nanozymes to remove more kinds of ROS, thus greatly improving the antioxidant treatment efficiency of nanozymes. In addition, nanozymes modified with other ligands, such as some proteins, plasmids, inhibitors, *etc.*, can achieve more functions.

Although the activity of SOD-like nanozymes has developed rapidly in recent years and the number of publications has increased rapidly, there still exist many problems. First, the catalytic mechanism of nanozymes to exert SOD-like activity is still unclear. At present, the development of SOD-like nanozymes mostly relies on random synthesis and screening, and few high-activity nanozymes are directly synthesized through rational design. Therefore, it is necessary to develop new methods and techniques to further explore the mechanism and active sites of nanozymes. Second, the activity of current SOD-like nanozymes is not satisfactory. To date, there are almost no nanozymes that can match the activity of natural SODs. Natural SOD enzymes enhance their substrate affinity through their fine structural regulation, so as to have high catalytic efficiency. However, although the structure of some nanozymes imitates the active sites of natural enzymes, their activity cannot exceed that of natural enzymes, and their structure–activity relationship is still not very thorough. Through in-depth exploration of the mechanism, nanozymes with a higher enzyme activity are expected to be developed. Third, the SOD-like activity determination method is not perfect. So far, the methods of SOD-like activity measurement are not uniform, and there is no uniform quantitative standard. Only qualitative comparison of several materials in the same study can be realized, and the activity of materials in different studies cannot be directly compared. Due to the different chemical nature of natural enzymes and nanozymes, some methods are not completely applicable to nanozymes although they are applicable to natural SODs. Therefore, new SOD-like activity determination methods and uniform measurement units for SOD-like nanozymes are expected to be established. In addition, due to the unknown active sites of nanozymes, most of the current methods are based on the weights of the materials, and the catalytic efficiency of each active site cannot be measured. Fourth, the application of SOD-like nanozymes

is limited. To date, the application of SOD-like nanozymes mainly focuses on the treatment of diseases in the antioxidant field, and some new suitable applications are expected to be explored. Fifth, some common problems of nanozymes remain to be solved, such as the specificity of enzyme activity, toxicity, metabolic problems and so on. At present, the most commonly used methods for the study of the biocompatibility and biosafety of nanozymes include histopathological staining, blood routine and blood biochemical testing to evaluate the potential impact of nanoparticles on body tissues. The results of animal experiments showed that cerium oxide,[61] carbon materials[48] and other nanozymes[126] exhibit good biocompatibility. In addition, a number of ultra-small nanozymes that can be cleared by the kidney have been designed.[114] However, the biocompatibility of most nanozymes is still a problem to be studied in depth. Most studies have not effectively evaluated the metabolic pathways of nanozymes. The potential effects of nanozymes on body tissues mainly include the following: firstly, after entering the organism, nanozymes may interact with biological components in the blood or cell fluid to form protein crowns, which may affect the catalytic activity of nanozymes on the one hand, and may cause biological safety issues on the other hand. Secondly, many nanozymes exhibit toxic peroxidase-like activity under acidic conditions, so some seemingly safe nanozyme materials may become toxic after entering the acid vesicles of cells. Thirdly, nanozymes may also interact with intracellular components such as proteins, nucleic acids and small biological molecules to disrupt their normal physiological functions. At present, there are few comprehensive studies on the biocompatibility mechanism of nanozymes, and further development of indicators for measuring their biocompatibility is needed.

In addition to the existing strategies for improving various existing nanozymes, it is a very promising strategy to directly create high-activity SOD-like nanozymes by imitating the active sites of natural enzymes. At present, there have been some studies on nanozymes imitating the natural enzyme active sites. For example, Patriarca *et al.* inserted a series of metal-center complexes into different kinds of mesoporous silica junctions, as shown in Fig. 16. For the 1 and 2 imidazolate complexes, the silica channels limited the geometry of the μ-imidazolate-Cu(II)$_2$ core and changed the relative orientations of the two copper coordination planes, resulting in a higher enzyme activity. Unlike imidazole bridging compounds, however, the insertion of 3 in mesoporous silica caused the hybrid material to become less stable, showing partial release into aqueous solution and dissociation, where the enzymatic activity of 3 is low. This was determined by the positional relationship between the active centers. This result was demonstrated by encapsulation with two different silica structures.[1,127] Another experiment combined different metal active center complexes into boehmite nanoparticles (BNPs). It was found that binuclear Cu^{2+} complexes showed a significant increase in SOD-like activity. This is because BNPs have positive ζ-potential, which helps drive $O_2^{\bullet -}$ to the active centers, consistent with the active sites of natural enzymes.[128] However, there are few studies on the use of natural enzyme active centers to guide the activity of nanozymes, and we look forward to the review of this article to provide more ideas for future. For example, the active centers of SOD are mostly composed of metal ions coordinated by C, N, O and other elements of surrounding amino acids. According to these coordination principles, nanozymes with SOD-like active center structures can be designed, such as some single atom nanozymes synthesized with MOFs and other materials as precursors. Some features of the catalytic microenvironment near the SOD active site may also be used to optimize nanozymes, such as cave shape, hydrophilicity, hydrophobicity, and charge properties. Moreover, the catalytic performance of SOD-like nanozymes may also be improved based on the simulation of the flexible metal-free frame architecture of the SOD active site.

Although there are still some problems in the development of SOD-like nanozymes, their advantages in replacing natural enzymes are nonnegligible. Nanozymes with SOD-like activity have wide application prospects. This review briefly introduces the development of SOD-like nanozymes, summarizes their mechanism, enzymatic activity and applications, and discusses their deficiencies in the current development, hoping to serve as a reference for future research. We expect that more SOD-like nanozymes with high activity will be developed and applied in a wider range of aspects.

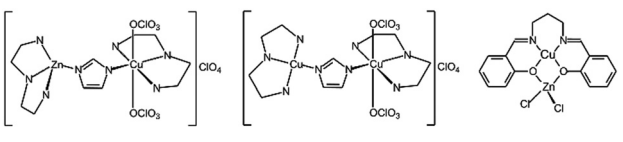

Fig. 16 Different metal-centre complexes were developed.[1] Reproduced with permission. Copyright 2020, Elsevier.

Author contributions

Hanqing Zhao: writing – original draft preparation. Ruofei Zhang: writing – review and editing. Xiyun Yan: supervision. Kelong Fan: conceptualization, supervision, writing – review and editing.

Conflicts of interest

There are no conflicts to declare.

Acknowledgements

This work was financially supported by the National Natural Science Foundation of China (No. 31900981), the Strategic Priority Research Program of CAS (XDB29040101), CAS Interdisciplinary Innovation Team (JCTD-2020-08), the Key Research Program of Frontier Sciences, CAS (Grant No. QYZDY-SSW-SMC013), and the Youth Innovation Promotion Association of Chinese Academy of Sciences (No. 2019093).

References

1 M. Patriarca, V. Daier, G. Cami, E. Riviere, C. Hureau and S. Signorella, *J. Inorg. Biochem.*, 2020, **207**, 111050.
2 S. Kang, Y. G. Gil, D. H. Min and H. Jang, *ACS Nano*, 2020, **14**, 4383–4394.
3 F. F. Cao, L. Zhang, Y. W. You, L. R. Zheng, J. S. Ren and X. G. Qu, *Angew. Chem., Int. Ed.*, 2020, **59**, 5108–5115.
4 S. S. Ali, J. I. Hardt, K. L. Quick, J. S. Kim-Han, B. F. Erlanger, T. T. Huang, C. J. Epstein and L. L. Dugan, *Free Radical Biol. Med.*, 2004, **37**, 1191–1202.
5 X. M. Shen, W. Q. Liu, X. J. Gao, Z. H. Lu, X. C. Wu and X. F. Gao, *J. Am. Chem. Soc.*, 2015, **137**, 15882–15891.
6 M. Ma, N. Gao, X. Li, Z. Liu, Z. Pi, X. Du, J. Ren and X. Qu, *ACS Nano*, 2020, **14**, 9894–9903.
7 X. Zhang, S. Lin, S. Liu, X. Tan, Y. Dai and F. Xia, *Coord. Chem. Rev.*, 2021, **429**, 213652.
8 N. Singh, M. A. Savanur, S. Srivastava, P. D'Silva and G. Mugesh, *Nanoscale*, 2019, **11**, 3855–3863.
9 V. Baldim, F. Bedioui, N. Mignet, I. Margaill and J. F. Berret, *Nanoscale*, 2018, **10**, 6971–6980.
10 C. Korsvik, S. Patil, S. Seal and W. T. Self, *Chem. Commun.*, 2007, 1056–1058, DOI: 10.1039/b615134e.
11 Z. Y. Yang, S. L. Luo, Y. P. Zeng, C. M. Shi and R. Li, *ACS Appl. Mater. Interfaces*, 2017, **9**, 6839–6848.
12 N. Singh, M. Geethika, S. M. Eswarappa and G. Mugesh, *Chem. – Eur. J.*, 2018, **24**, 8393–8403.
13 J. He, L. Zhou, J. Liu, L. Yang, L. Zou, J. Y. Xiang, S. W. Dong and X. C. Yang, *Appl. Surf. Sci.*, 2017, **402**, 469–477.
14 S. B. Guo and L. Guo, *J. Phys. Chem. C*, 2019, **123**, 30318–30334.
15 L. Baud and R. Ardaillou, *Am. J. Physiol.*, 1986, **251**, F765–F776.
16 C. Liu, Y. Y. Yan, X. W. Zhang, Y. Y. Mao, X. Q. Ren, C. Y. Hu, W. W. He and J. J. Yin, *Nanoscale*, 2020, **12**, 3068–3075.
17 B. H. San, S. H. Moh and K. K. Kim, *J. Mater. Chem.*, 2012, **22**, 1774–1780.
18 S. Barkam, J. Ortiz, S. Saraf, N. Eliason, R. Mccormack, S. Das, A. Gupta, C. Neal, A. Petrovic, C. Hansor, M. D. Sevilla, A. Adhikary and S. Seal, *J. Phys. Chem. C*, 2017, **121**, 20039–20050.
19 D. M. Miller, G. R. Buettner and S. D. Aust, *Free Radical Biol. Med.*, 1990, **8**, 95–108.
20 M. Valko, H. Morris and M. T. D. Cronin, *Curr. Med. Chem.*, 2005, **12**, 1161–1208.
21 M. Valko, D. Leibfritz, J. Moncol, M. T. D. Cronin, M. Mazur and J. Telser, *Int. J. Biochem. Cell Biol.*, 2007, **39**, 44–84.
22 W. Wang, X. P. Jiang and K. Z. Chen, *Chem. Commun.*, 2012, **48**, 7289–7291.
23 I. Fridovich, *Photochem. Photobiol.*, 1978, **28**, 733–741.
24 I. A. Abreu and D. E. Cabelli, *Biochim. Biophys. Acta, Proteins Proteomics*, 2010, **1804**, 263–274.
25 M. A. Damle, A. P. Jakhade and R. C. Chikate, *ACS Omega*, 2019, **4**, 3761–3771.
26 L. Z. Gao, J. Zhuang, L. Nie, J. B. Zhang, Y. Zhang, N. Gu, T. H. Wang, J. Feng, D. L. Yang, S. Perrett and X. Yan, *Nat. Nanotechnol.*, 2007, **2**, 577–583.
27 K. M. Beem, W. E. Rich and K. V. Rajagopalan, *J. Biol. Chem.*, 1974, **249**, 7298–7305.
28 M. A. Hough and S. S. Hasnain, *Structure*, 2003, **11**, 937–946.
29 J. S. Richardson, K. A. Thomas, B. H. Rubin and D. C. Richardson, *Proc. Natl. Acad. Sci. U. S. A.*, 1975, **72**, 1349–1353.
30 N. Boden, M. C. Holmes and P. F. Knowles, *Biochem. Biophys. Res. Commun.*, 1974, **57**, 845–848.
31 I. Fridovich, *Annu. Rev. Biochem.*, 1975, **44**, 147–159.
32 C. L. Fisher, D. E. Cabelli, J. A. Tainer, R. A. Hallewell and E. D. Getzoff, *Proteins: Struct., Funct., Genet.*, 1994, **19**, 24–34.
33 E. D. Getzoff, D. E. Cabelli, C. L. Fisher, H. E. Parge, M. S. Viezzoli, L. Banci and R. A. Hallewell, *Nature*, 1992, **358**, 347–351.
34 L. M. Ellerby, D. E. Cabelli, J. A. Graden and J. S. Valentine, *J. Am. Chem. Soc.*, 1996, **118**, 6556–6561.
35 J. Azadmanesh, S. R. Trickel and G. E. O. Borgstahl, *J. Struct. Biol.*, 2017, **199**, 68–75.
36 J. Azadmanesh and G. E. O. Borgstahl, *Antioxidants*, 2018, **7**, 16.
37 M. S. Lah, M. M. Dixon, K. A. Pattridge, W. C. Stallings, J. A. Fee and M. L. Ludwig, *Biochemistry*, 1995, **34**, 1646–1660.
38 J. Shearer, *Acc. Chem. Res.*, 2014, **47**, 2332–2341.
39 H. W. Kroto, J. R. Heath, S. C. Obrien, R. F. Curl and R. E. Smalley, *Nature*, 1985, **318**, 162–163.
40 S. Torbruegge, M. Reichling, A. Ishiyama, S. Morita and O. Custance, *Phys. Rev. Lett.*, 2007, **99**, 056101.
41 E. G. Heckert, A. S. Karakoti, S. Seal and W. T. Self, *Biomaterials*, 2008, **29**, 2705–2709.
42 A. Vincent, S. Babu, E. Heckert, J. Dowding, S. M. Hirst, T. M. Inerbaev, W. T. Self, C. M. Reilly, A. E. Masunov, T. S. Rahman and S. Seal, *ACS Nano*, 2009, **3**, 1203–1211.
43 X. L. Ren, X. W. Meng, J. Ren and F. Q. Tang, *RSC Adv.*, 2016, **6**, 92839–92844.
44 Y. S. Yang, Z. Mao, W. J. Huang, L. H. Liu, J. L. Li and Q. Z. Wu, *Sci. Rep.*, 2016, **6**, 7.
45 B. Bhushan and P. Gopinath, *J. Mater. Chem. B*, 2015, **3**, 4843–4852.
46 L. L. Dugan, J. K. Gabrielsen, S. P. Yu, T. S. Lin and D. W. Choi, *Neurobiol. Dis.*, 1996, **3**, 129–135.
47 S. S. Ali, J. I. Hardt and L. L. Dugan, *Nanomedicine*, 2008, **4**, 283–294.
48 K. L. Fan, J. Q. Xi, L. Fan, P. X. Wang, C. H. Zhu, Y. Tang, X. D. Xu, M. M. Liang, B. Jiang, X. Y. Yan and L. Z. Gao, *Nat. Commun.*, 2018, **9**, 11.
49 J. Q. Xi, G. Wei, Q. W. Wu, Z. L. Xu, Y. W. Liu, J. Han, L. Fan and L. Z. Gao, *Biomater. Sci.*, 2019, **7**, 4131–4141.
50 J. Kim, M. Takahashi, T. Shimizu, T. Shirasawa, M. Kajita, A. Kanayama and Y. Miyamoto, *Mech. Ageing Dev.*, 2008, **129**, 322–331.
51 W. W. He, Y. T. Zhou, W. G. Warner, X. N. Hu, X. C. Wu, Z. Zheng, M. D. Boudreau and J. J. Yin, *Biomaterials*, 2013, **34**, 765–773.
52 K. Korschelt, R. Ragg, C. S. Metzger, M. Kluenker, M. Oster, B. Barton, M. Panthofer, D. Strand, U. Kolb, M. Mondeshki, S. Strand, J. Brieger, M. N. Tahir and W. Tremel, *Nanoscale*, 2017, **9**, 3952–3960.

53 D. Lieb, I. Kenkell, J. L. Miljkovic, D. Moldenhauer, N. Weber, M. R. Filipovic, F. Grohn and I. Ivanovic-Burmazovic, *Inorg. Chem.*, 2014, **53**, 1009–1020.
54 J. S. Mu, X. Zhao, J. Li, E. C. Yang and X. J. Zhao, *J. Mater. Chem. B*, 2016, **4**, 5217–5221.
55 J. L. Dong, L. N. Song, J. J. Yin, W. W. He, Y. H. Wu, N. Gu and Y. Zhang, *ACS Appl. Mater. Interfaces*, 2014, **6**, 1959–1970.
56 T. M. Chen, H. Zou, X. J. Wu, C. C. Liu, B. Situ, L. Zheng and G. W. Yang, *ACS Appl. Mater. Interfaces*, 2018, **10**, 12453–12462.
57 Z. H. Miao, S. S. Jiang, M. L. Ding, S. Y. Sun, Y. Ma, M. R. Younis, G. He, J. G. Wang, J. Lin, Z. Cao, P. Huang and Z. B. Zha, *Nano Lett.*, 2020, **20**, 3079–3089.
58 S. Sahar, A. Zeb, C. Ling, A. Raja, G. Wang, N. Ullah, X. M. Lin and A. W. Xu, *ACS Nano*, 2020, **14**, 3017–3031.
59 M. Kajita, K. Hikosaka, M. Iitsuka, A. Kanayama, N. Toshima and Y. Miyamoto, *Free Radicals Res.*, 2007, **41**, 615–626.
60 Z. Moradi-Shoeili, *React. Kinet., Mech. Catal.*, 2017, **120**, 323–332.
61 V. Singh, S. Singh, S. Das, A. Kumar, W. T. Self and S. Seal, *Nanoscale*, 2012, **4**, 2597–2605.
62 E. L. G. Samuel, D. C. Marcano, V. Berka, B. R. Bitner, G. Wu, A. Potter, R. H. Fabian, R. G. Pautler, T. A. Kent, A. L. Tsai and J. M. Tour, *Proc. Natl. Acad. Sci. U. S. A.*, 2015, **112**, 2343–2348.
63 J. D. Weaver and C. L. Stabler, *Acta Biomater.*, 2015, **16**, 136–144.
64 S. B. Guo, Y. Han and L. Guo, *Catal. Surv. Asia*, 2020, **24**, 70–85.
65 Y. Han, Z. J. Zhang and L. Guo, *Catal. Surv. Asia*, 2020, **24**, 166–177.
66 N. Singh, M. A. Savanur, S. Srivastava, P. D'Silva and G. Mugesh, *Angew. Chem., Int. Ed.*, 2017, **56**, 14267–14271.
67 J. Yao, Y. Cheng, M. Zhou, S. Zhao, S. C. Lin, X. Y. Wang, J. J. X. Wu, S. R. Li and H. Wei, *Chem. Sci.*, 2018, **9**, 2927–2933.
68 A. Gupta, S. Das, C. J. Neal and S. Seal, *J. Mater. Chem. B*, 2016, **4**, 3195–3202.
69 V. Baldim, N. Yadav, N. Bia, A. Graillot, C. Loubat, S. Singh, A. S. Karakoti and J.-F. Berret, *ACS Appl. Mater. Interfaces*, 2020, **12**, 42056–42066.
70 V. Jain, S. Bhagat, M. Singh, V. Bansal and S. Singh, *RSC Adv.*, 2019, **9**, 33195–33206.
71 X. H. Chen, W. Jiang, Q. R. Cheng, Z. Q. Pan and H. Zhou, *Micro Nano Lett.*, 2014, **9**, 157–161.
72 V. Patel, M. Singh, E. L. H. Mayes, A. Martinez, V. Shutthanandan, V. Bansal, S. Singh and A. S. Karakoti, *Chem. Commun.*, 2018, **54**, 13973–13976.
73 Y. Liu, H. H. Wu, M. Li, J. J. Yin and Z. H. Nie, *Nanoscale*, 2014, **6**, 11904–11910.
74 S. Singh, T. Dosani, A. S. Karakoti, A. Kumar, S. Seal and W. T. Self, *Biomaterials*, 2011, **32**, 6745–6753.
75 U. Carmona, L. B. Zhang, L. Li, W. Munchgesang, E. Pippel and M. Knez, *Chem. Commun.*, 2014, **50**, 701–703.
76 X. L. Ren, M. Q. Wang, X. He, Z. Li, J. Zhang, W. Zhang, X. D. Chen, H. Ren and X. W. Meng, *Chin. Chem. Lett.*, 2018, **29**, 1865–1868.
77 L. Huang, Y. S. Niu, R. G. Li, H. Z. Liu, Y. Wang, G. F. Xu, Y. Li and Y. H. Xu, *Anal. Chem.*, 2019, **91**, 5753–5761.
78 G. Wu, V. Berka, P. J. Derry, K. Mendoza, E. Kakadiaris, T. Roy, T. A. Kent, J. M. Tour and A. L. Tsai, *ACS Nano*, 2019, **13**, 11203–11213.
79 Z. Liu, L. N. Xie, K. Q. Qiu, X. X. Liao, T. W. Rees, Z. Z. Zhao, L. N. Ji and H. Chao, *ACS Appl. Mater. Interfaces*, 2020, **12**, 31205–31216.
80 M. M. Sozarukova, M. A. Shestakova, M. A. Teplonogova, D. Y. Izmailov, E. V. Proskurnina and V. K. Ivanov, *Russ. J. Inorg. Chem.*, 2020, **65**, 597–605.
81 R. W. Zhou, P. Y. Wang, Y. R. Guo, X. F. Dai, S. Q. Xiao, Z. Fang, R. Speight, E. W. W. Thompson, P. J. Cullen and K. Ostrikov, *Nanoscale*, 2019, **11**, 19497–19505.
82 F. Dashtestani, H. Ghourchian and A. Najafi, *Bioorg. Chem.*, 2018, **80**, 621–630.
83 D. R. Bohn, F. O. Lobato, A. S. Thill, L. Steffens, M. Raabe, B. Donida, C. R. Vargas, D. J. Moura, F. Bernardi and F. Poletto, *J. Mater. Chem. B*, 2018, **6**, 4920–4928.
84 Y. Liu, Y. Zhang, Q. Liu, Q. Wang, A. Lin, J. Luo, Y. Du, Y.-W. Lin and H. Wei, *Analyst*, 2021, **146**, 1872–1879.
85 N. Higashi, T. Shosu, T. Koga, M. Niwa and T. Tanigawa, *J. Colloid Interface Sci.*, 2006, **298**, 118–123.
86 P. Witte, F. Beuerle, U. Hartnagel, R. Lebovitz, A. Savouchkina, S. Sali, D. Guldi, N. Chronakis and A. Hirsch, *Org. Biomol. Chem.*, 2007, **5**, 3599–3613.
87 V. K. Klochkov, A. V. Grigorova, O. O. Sedyh and Y. V. Malyukin, *Colloids Surf., A*, 2012, **409**, 176–182.
88 R. N. McCormack, P. Mendez, S. Barkam, C. J. Neal, S. Das and S. Seal, *J. Phys. Chem. C*, 2014, **118**, 18992–19006.
89 M. Yang, W. Jiang, Z. Q. Pan and H. Zhou, *J. Inorg. Organomet. Polym.*, 2015, **25**, 1289–1297.
90 R. Ragg, A. M. Schilmann, K. Korschelt, C. Wieseotte, M. Kluenker, M. Viel, L. Volker, S. Preiss, J. Herzberger, H. Frey, K. Heinze, P. Blumler, M. N. Tahir, F. Natalio and W. Tremel, *J. Mater. Chem. B*, 2016, **4**, 7423–7428.
91 T. Naganuma, *Nano Res.*, 2017, **10**, 199–217.
92 Y. Pan, Y. M. Wang, X. Y. Fan, W. B. Wang, X. M. Yang, D. Z. Cui and M. Zhao, *Environ. Microbiol. Rep.*, 2019, **11**, 140–146.
93 X. Cai, Q. M. Gao, S. H. Zuo, H. L. Zhao and M. B. Lan, *Electroanalysis*, 2020, **32**, 598–605.
94 X. M. Jiang, P. Gray, M. Patel, J. W. Zheng and J. J. Yin, *J. Mater. Chem. B*, 2020, **8**, 1191–1201.
95 I. V. Mikheev, M. M. Sozarukova, E. V. Proskurnina, I. E. Kareev and M. A. Proskurnin, *Molecules*, 2020, **25**, 2506.
96 S. C. Lin, Y. Cheng, H. Zhang, X. Y. Wang, Y. Y. Zhang, Y. J. Zhang, L. Y. Miao, X. Z. Zhao and H. Wei, *Small*, 2020, **15**, 1902123.
97 V. Nicolini, G. Malavasi, G. Lusvardi, A. Zambon, F. Benedetti, G. Cerrato, S. Valeri and P. Luches, *Ceram. Int.*, 2019, **45**, 20910–20920.
98 K. Kamada and N. Soh, *J. Phys. Chem. B*, 2015, **119**, 5309–5314.
99 F. M. Ribeiro, M. M. de Oliveira, S. Singh, T. S. Sakthivel, C. J. Neal, S. Seal, T. Ueda-Nakamura, S. d. O. Silva

Lautenschlager and C. V. Nakamura, *Front. Bioeng. Biotechnol.*, 2020, **8**, 577557.
100 C. X. Ren, D. D. Li, Q. X. Zhou and X. G. Hu, *Biomaterials*, 2020, **232**, 119752.
101 D. Q. Yu, M. M. Ma, Z. W. Liu, Z. F. Pi, X. B. Du, J. S. Ren and X. G. Qu, *Biomaterials*, 2020, **255**, 10.
102 Y. H. Gu, Y. X. Huang, Z. Y. Qiu, Z. B. Xu, D. D. Li, L. Chen, J. Jiang and L. Z. Gao, *Sci. China: Life Sci.*, 2020, **63**, 68–79.
103 H. Li, J. Yan, D. Meng, R. Cai, X. Gao, Y. Ji, L. Wang, C. Chen and X. Wu, *ACS Nano*, 2020, **14**, 12854–12865.
104 P. Allawadhi, A. Khurana, S. Allwadhi, K. Joshi, G. Packirisamy and K. K. Bharani, *Nano Today*, 2020, **35**, 100982.
105 Y. Chen, J. B. Tan, Q. Zhang, T. Xin, Y. L. Yu, Y. Nie and S. Y. Zhang, *Nano Lett.*, 2020, **20**, 6548–6555.
106 J. L. Zhao, W. Gao, X. J. Cai, J. J. Xu, D. W. Zou, Z. S. Li, B. Hu and Y. Y. Zheng, *Theranostics*, 2019, **9**, 2843–2855.
107 L. Y. Wu, G. Y. Liu, W. Y. Wang, R. B. Liu, L. Y. Liao, N. Cheng, W. T. Li, W. F. Zhang and D. J. Ding, *Int. J. Nanomed.*, 2020, **15**, 2515–2527.
108 W. Li, Z. Liu, C. Q. Liu, Y. J. Guan, J. S. Ren and X. G. Qu, *Angew. Chem., Int. Ed.*, 2017, **56**, 13661–13665.
109 F. Dashtestani, H. Ghourchian and A. Najafi, *Mater. Sci. Eng., C*, 2019, **94**, 831–840.
110 X. Cai, L. B. Shi, W. Q. Sun, H. L. Zhao, H. Li, H. Y. He and M. B. Lan, *Biosens. Bioelectron.*, 2018, **102**, 171–178.
111 Y. J. Sang, F. F. Cao, W. Li, L. Zhang, Y. W. You, Q. Q. Deng, K. Dong, J. S. Ren and X. G. Qu, *J. Am. Chem. Soc.*, 2020, **142**, 5177–5183.
112 Y. F. Liu, Y. Cheng, H. Zhang, M. Zhou, Y. J. Yu, S. C. Lin, B. Jiang, X. Z. Zhao, L. Y. Miao, C. W. Wei, Q. Y. Liu, Y. W. Lin, Y. Du, C. J. Butch and H. Wei, *Sci. Adv.*, 2020, **6**, 10.
113 J. Liu, W. Zhang, M. H. Peng, G. Y. Ren, L. H. Guan, K. Li and Y. Q. Lin, *ACS Appl. Mater. Interfaces*, 2020, **12**, 29631–29640.
114 T. F. Liu, B. W. Xiao, F. Xiang, J. L. Tan, Z. Chen, X. R. Zhang, C. Z. Wu, Z. W. Mao, G. X. Luo, X. Y. Chen and J. Deng, *Nat. Commun.*, 2020, **11**, 16.
115 S. Singh, R. Asal and S. Bhagat, *J. Biomed. Mater. Res., Part A*, 2018, **106**, 3152–3164.
116 M. Cui, J. J. Ren, X. F. Wen, N. Li, Y. F. Xing, C. Zhang, Y. Y. Han and X. P. Ji, *Chem. Res. Chin. Univ.*, 2020, **36**, 774–780.
117 R. J. Yan, S. Sun, J. Yang, W. Long, J. Y. Wang, X. Y. Mu, Q. F. Li, W. T. Hao, S. F. Zhang, H. L. Liu, Y. L. Gao, L. F. Ouyang, J. C. Chen, S. J. Liu, X. D. Zhang and D. Ming, *ACS Nano*, 2019, **13**, 11552–11560.
118 L. Zhang, Y. Zhang, Z. Z. Wang, F. F. Cao, Y. J. Sang, K. Dong, F. Pu, J. S. Ren and X. G. Qu, *Mater. Horiz.*, 2019, **6**, 1682–1687.
119 A. Khurana, P. Anchi, P. Allawadhi, V. Kumar, N. Sayed, G. Packirisamy and C. Godugu, *Nanomedicine*, 2019, **14**, 1805–1825.
120 Q. S. Han, X. H. Wang, X. L. Liu, Y. F. Zhang, S. F. Cai, C. Qi, C. Wang and R. Yang, *J. Colloid Interface Sci.*, 2019, **539**, 575–584.
121 C. L. Hao, A. H. Qu, L. G. Xu, M. Z. Sun, H. Y. Zhang, C. L. Xu and H. Kuang, *J. Am. Chem. Soc.*, 2019, **141**, 1091–1099.
122 H. A. Rather, R. Thakore, R. Singh, D. Jhala, S. Singh and R. Vasita, *Bioact. Mater.*, 2018, **3**, 201–211.
123 Y. Wang, M. Q. Wang, L. L. Lei, Z. Y. Chen, Y. S. Liu and S. J. Bao, *Microchim. Acta*, 2018, **185**, 140.
124 P. Jawaid, M. U. Rehman, Q. L. Zhao, K. Takeda, K. Ishikawa, M. Hori, T. Shimizu and T. Kondo, *J. Cell. Mol. Med.*, 2016, **20**, 1737–1748.
125 W. F. Zheng, B. Jiang, Y. Hao, Y. Y. Zhao, W. Zhang and X. Y. Jiang, *Biofabrication*, 2014, **6**, 045004.
126 Q. X. Zhang, H. Tao, Y. Y. Lin, Y. Hu, H. J. An, D. L. Zhang, S. B. Feng, H. Y. Hu, R. B. Wang, X. H. Li and J. X. Zhang, *Biomaterials*, 2016, **105**, 206–221.
127 M. Patriarca, V. Daier, G. Cami, N. Pellegri, E. Riviere, C. Hureau and S. Signorell, *Microporous Mesoporous Mater.*, 2019, **279**, 133–141.
128 A. Martinez-Camarena, J. M. Linares, A. Domenech-Carbo, J. Alarcon and E. Garcia-Espana, *RSC Adv.*, 2019, **9**, 41549–41560.